CFD SIMULATION AND ANALYSIS OF TWISTED TAPE INSERTED PARABOLIC SOLAR COLLECTOR THERMAL PERFORMANCE

2023
MASTER THESIS
MECHANICAL ENGINEERING

Nasseer Sabbeeh Jaralleh AL NUSEEIRY

Thesis Advisor
Assoc. Prof. Dr. Selçuk SELİMLİ

CFD SIMULATION AND ANALYSIS OF TWISTED TAPE INSERTED PARABOLIC SOLAR COLLECTOR THERMAL PERFORMANCE

Nasseer Sabbeeh Jaralleh AL NUSEEIRY

Thesis Advisor

Assoc. Prof. Dr. Selçuk SELİMLİ

T.C.

Karabuk University

Institute of Graduate Programs

Department of Mechanical Engineering

Prepared as

Master Thesis

KARABUK

February 2023

I certify that in my opinion the thesis submitted by Nasseer Sabbeeh Jaralleh AL NUSEEIRY titled "CFD SIMULATION AND ANALYSIS OF TWISTED TAPE INSERTED PARABOLIC SOLAR COLLECTOR THERMAL PERFORMANCE" is fully adequate in scope and in quality as a thesis for the degree of Master of Science.

Assoc. Prof. Dr. Selçuk SELİMLİ .....
Thesis Advisor, Department of Energy Systems Engineering

This thesis is accepted by the examining committee with a unanimous vote in the Department of Mechanical Engineering as a Master of Science thesis. 15/02/2023

Examining Committee Members (Institutions)	Signature
Chairman : Prof. Dr. Mustafa AKTAŞ (GU)	.....
Member : Assoc. Prof. Dr. Selçuk SELİMLİ (KBU)	.....
Member : Assist. Prof. Dr. Enes KILINÇ (KBU)	.....

The degree of Master of Science by the thesis submitted is approved by the Administrative Board of the Institute of Graduate Programs, Karabuk University.

Prof. Dr. Müslüm KUZU .....
Director of the Institute of Graduate Programs

"I declare that all the information within this thesis has been gathered and presented in accordance with academic regulations and ethical principles and I have according to the requirements of these regulations and principles cited all those which do not originate in this work as well."

Nasseer Sabbeeh Jaralleh AL NUSEEIRY

ABSTRACT

M. Sc. Thesis

CFD SIMULATION AND ANALYSIS OF TWISTED TAPE INSERTED PARABOLIC SOLAR COLLECTOR THERMAL PERFORMANCE

Nasseer Sabbeeh Jaralleh AL NUSEEIRY

Karabük University
Institute of Graduate Programs
The Department of Mechanical Engineering

Thesis Advisor:
Assoc. Prof. Dr. Selcuk SELİMLİ
February 2023, 83 pages

Parabolic through solar collectors are renewable systems whose usage areas are expanding, and development activities continue with interest. In particular, parabolic corrugated collectors for low enthalpy processes are an emerging technology. Recently, many applications and research studies have been carried out for the development of these systems. One technique to achieve this is to increase heat transfer by placing a twisted tape on the receiving tube. Improving the transfer of the reflected solar power to the fluid in the absorber tube by collecting in the parabolic concentrator to the absorber tube, where the water flow is provided; The twisted tape with y/w= (2,4 and 6) was positioned on the tube and investigated with a computer-based simulation study. The results showed that the Nusselt number, mean pressure, friction factor, and thermal efficiency increased in the presence of a twist splice compared to the empty tube. Nusselt number, friction factor and thermal efficiency increase for Re (500, 1000, and 1500) values compared to empty tube for y/w=2 twisted tape

application (73%, 82% and 17%), (83%, 85%) respectively and 19%), (87%, 87% and 21%). For twisted tape application with y/w=4 (Nusselt number, friction factor and thermal efficiency) increase (61%,72%, and 11%) (75%,76%, and 14%), (81%,78%) %, and 15%). The increase obtained for the twisted strip application with y/w=6 was (53%,70%, and 7%) (69%,73%, and 12%), (76%,75%, and 13%).

Key Words : Nusselt number, thermal efficiency, solar collector, parabolic trough solar collector, heat transfer, Reynolds number.

Science Code : 91408

ÖZET

Yüksek Lisans Tezi

BÜKÜMLÜ BANT YERLEŞTİRİLEN PARABOLİK GÜNEŞ KOLLEKTÖRÜ TERMAL PERFORMANSININ CFD SİMÜLASYONU VE ANALİZİ

Nasseer Sabbeeh Jaralleh AL NUSEEIRY

Karabük Üniversitesi
Lisansüstü Eğitim Enstitüsü
Makine Mühendisliği Anabilim Dalı

Tez Danışmanı:
Doç. Dr. Selçuk SELİMLİ
Şubat 2023, 83 sayfa

Parabolik oluklu güneş kolektörleri günümüzde kullanım alanları genişleyen ve geliştirme faaliyetleri ilgiyle devam eden yenilenebilir sistemlerdir. Özellikle, düşük entalpili prosesler için parabolik oluklu toplayıcılar gelişmekte olan bir teknolojidir. Son zamanlarda bu sistemlerin geliştirilmesine yönelik birçok hem uygulama hem de araştırma çalışması yapılmaktadır. Bunu başarmanın bir tekniği de alıcı tüpe bükümlü bir bant yerleştirerek ısı transferini artırmaktır. Su akışı sağlanan soğurucu tüpe parabolik yoğunlaştırıcıda toplanarak yansıtılan güneş gücünün soğurucu tüpte akışkana aktarımının iyileştirilmesi; tüpe y/w= (2,4 ve 6) olan bükümlü bant konumlandırılarak yapılan bilgisayar tabanlı simülasyon çalışması ile incelenmiştir. Elde edilen sonuçlar, bükümlü bir bant ekinin varlığında boş tüpe kıyasla Nusselt sayısının, ortalama basıncın, sürtünme faktörünün ve termal verimliliğin arttığını göstermiştir. y/w=2 bükümlü bant uygulaması için boş tüpe kıyasla Re (500,1000, and 1500) değerleri için Nusselt sayısı, sürtünme faktörü ve termal verim artışı Sırasıyla

(%73, %82 ve %17), (%83, %85 ve %19), (%87, %87 ve %21)'dır. y/w=4 olan bükümlü bant uygulaması için (Nusselt sayısı, sürtünme faktörü ve termal verim) artışı sırasıyla (61%,72%, and 11%) (75%,76%, and 14%), (81%,78%, and 15%)'dır. y/w=6 olan bükümlü şerit uygulaması için elde edilen artış (53%,70%, and 7%) (69%,73%, and 12%), (76%,75%, and 13%) olarak belirlenmiştir.

Anahtar Kelimeler : Nusselt sayısı, ısıl verim, güneş kollektörü, parabolik oluk güneş kollektörü, ısı transferi, Reynolds sayısı.

Bilim Kodu **:** 91408

ACKNOWLEDGMENT

First of all, I thank God Almighty for everything. I would like to express my sincere thanks, appreciation, and gratitude to Assoc. Prof. Dr. Selcuk SELİMLİ for his time, expertise, support, guidance, and interest in supervising my thesis, ask God Almighty to reward him with the best reward. I also thank the head of the department of mechanical engineering, Prof. Dr. Kamil ARSLAN, and his staff for the assistance and guidance they have given us. My thanks and gratitude to eng. Hyder Mohee Razzouqi for his assist and support, wishing the best ranks and success. I dedicate this thesis to my beloved father and dear mother, my dear brothers and sisters, my dear wife and children, my dear colleagues and friends, to those who supported me, wishing them the best ranks and success. Finally, I can only pray to God Almighty to grant us guidance, chastity, wealth, health, safety, and who inspires me with more determination and strength to upgrade my scientific thesis.

CONTENTS

Page

Page

Page

LIST OF FIGURES

Page

LIST OF TABLES

Page

SYMBOLS AND ABBREVITIONS

SYMBOLS

α_r	: Absorptivity for an absorber tube
A_a	: Aperture area
W_a	: Aperture width
$C_o = A_a/A_r$	: Concentration ratio
ε	: Emissivity
D_o	: External diameter
f	: Focal length
U_L	: Global loss coefficient
D_i	: Internal diameter
L	: Length of the parabolic reflector
h_r	: Linearized radiation coefficient
Nu	: Nusselts number
η_o	: Optical efficiency
PTC	: Parabolic trough collector
Re	: Reynolds number
A_r	: Receiver area
ρ	: Reflectivity for a parabolic mirror
ϕ	: Rim angle
C_P	: Specific heat at constant pressure
w	: Tape width
y	: Tape pitch length
η_I	: Thermal efficiency
α_w	: Thermal diffusivity
K	: Thermal conductivity
k_{air}	: Thermal conductivity
k_w	: Thermal conductivity

y/w : Twist ratio

ρ_w : Water density

μ_w : Water dynamic viscosity

C_{pw} : Water heat capacity

v_w : Water kinematic viscosity

v_{air} : Water kinematic viscosity

h_v : Wind losses coefficient

PART 1

INTRODUCTION

1.1. RENEWABLE ENERGY

The renewable energy topic concerns professionals as well as to the common public increasingly. The investigations on the sources of renewable energy increased in the last period in the relative and absolute subjects. The renewable energy can implement an important base through treating the depletion fossil fuel issues and global heating. Fossil fuels, renewable resources and nuclear resources are the main energy sources [1]. The renewable energies sources as solar, geothermal, hydro-power, biomass and wind are used to re-produce energy and are useful extensively for combating crises of energy [2]. Renewable energy resources are represented the clean energy resources and critically important as a result of their friendly natures of environment [3]. Dependence on fossil fuels have resulted for environment pollution, carbon dioxide emissions and problems of greenhouse gas [4,5]. Renewable energy source can meet requirements of energy with the latent for supplying energy services with none emission of air pollutants and greenhouse gases [6,7]. Sustainable growth of remote zones in the desert and mountain regions [7–9]. There is currently an universal tendency to change fossil fuels with renewable energy source to achieve the excessive energy demand [10]. There are several challenges such as carbon dioxide emissions greenhouse gasses emissions, energy security and climate change that have lead in renewable energy seeking to meet a developing need in environment in present [11,12]. Continuous flow of clean and secure energy is essential which has smaller environmental influents to fulfil sustainable growth [13]. Major shift in energy forms is required to fulfil sustainable development without damaging climate system [14]. Although the renewable energy ration of universal energy consumption are little, but technologies of renewable energy are developing continuously and being spread rapidly [13].

1.1.1. Solar Energy

Solar energy can be used out of photocatalytic, photovoltaic and photo-thermal means. Photo-electrochemical converting solar energy into chemical energy and fuels, by photocatalytic chemical synthesis and artificial photosynthesis this themed issue on advances in solar energy converting brings together professionals in this range to characterized current researches and future prospects in this field [15]. At having a closer look at technologies of renewable and their last development statistics, it can be noted an incredibly interesting in solar-powered systems, with almost 60% of the renewable's overall capacity developed in 2019 of 98 GW, as illustrated in Figure 1.1 [16].

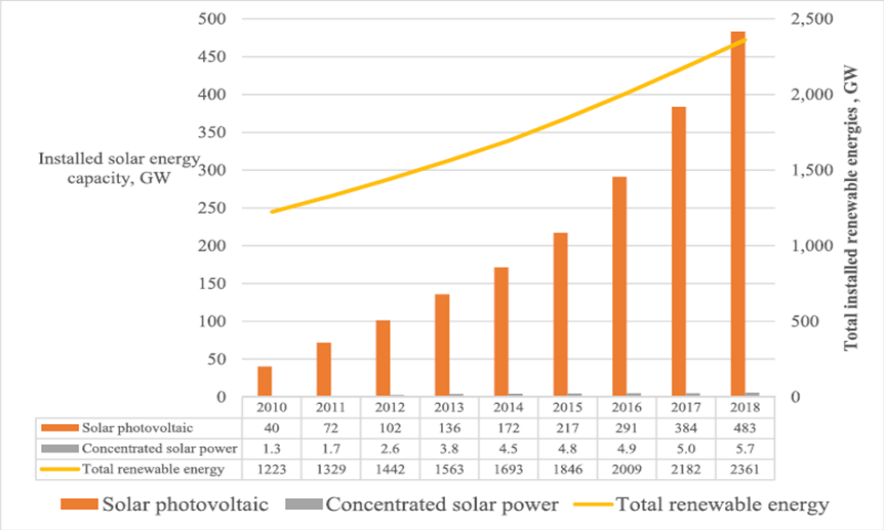

Figure 1.1. Installed capacity trends of solar energy and all renewable energy systems [16].

The energy from the sun can be used essentially out of three ways as shown in Figure 1.2 [17].

- Generating chemical fuel through artificial photosynthesis.
- Producing electricity from exciting electrons in the solar cell.
- Focus sunlight for producing heat.

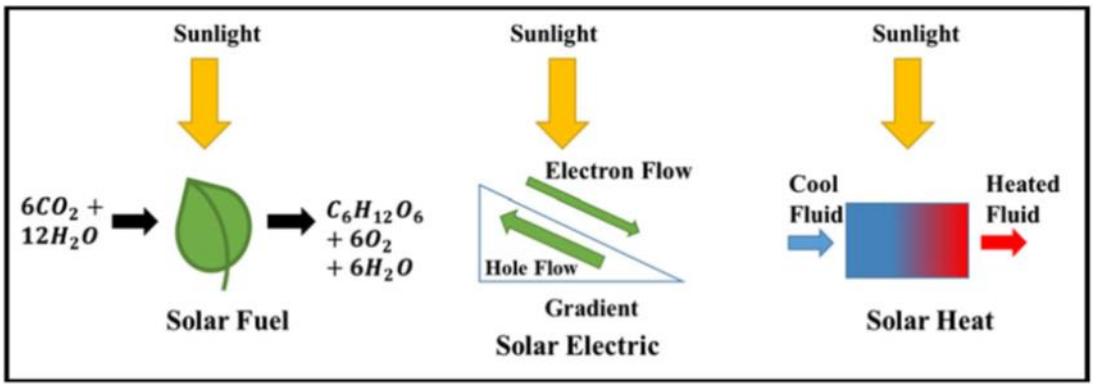

Figure 1.2. Three ways of converting solar energy into other forms of energy [17].

In general, solar energy is currently used in very small as (0.015) percent is utilized for generating electricity, (0.3) percent for heating and (11) percent of solar energy is used in naturalistic photosynthesis of biomass. be that as it may about (80%-85%) of the universal energy demands are meet utilizing fossil fuels. The fossil fuels problem is that their reserves exhaustible and not environment friend, result of the carbon dioxide emission. One ton of carbon dioxide is released into the atmosphere for every ton of coal burned. This emission is extremely harmful to the environment and is the primary cause of the greenhouse effect and the ozone layer's thinning, universal warming and climate change [17]. It is approximated that (90%) of the energy is produced at (0 to 0.23 of R, where R is sun radius), which include (40%) of the sun mass. At 0.7 of R from the centre, the temperature has decline to about 130,000K and the density has decline to (70 kg/m^3), here processes of convection begin to become significant, and the region from (0.7 to 1.0) R is fame as the convective zone. Within this region the temperature declines to about (5000 K) and the density declines to about (10^{-5} kg/m^3) [18]. Time of solar is the time utilize in whole relationships of the sun angle, it does not synchronize with local clock time. It is needful to convert standard time to solar time by employing two corrections. First, by using a constant correction for the variation in longitude between the observer of meridian, known as longitude, and the meridian on which the local standard time is depended the sun takes four minute to cross-cut one degree of longitude. The second correction is taken from the equation of time, which considered the perturbations in the earth rotation rate, which impact the time the sun crosses the observer meridian [18].

1.2. SOLAR COLLECTOR

Solar collectors are the key constituent of solar heating systems. The sun energy is collected and convert its radiation to the heat, then that heat is transferred to a fluid. The solar thermal energy can be utilized in solar space-heating systems, solar water-heating systems and solar pool heaters [19]. Solar thermal collectors considered one of the principle methods of extracting energy, which different drastically in the amount of solar flux captured in addition to the way for capture [20]. The most popular type of the solar thermal collector uses an absorber black surface, which then transfers heat to the working fluid in the tubes constructed within or melted onto the surface. In this case the efficiency is restricted by not only by active the absorber captures solar energy but also by actively the heat transferred to the fluid. The way that has been applied to enhance the efficiency of collectors while simplifying the system is to absorb the solar energy directly through the fluid volume, which known as direct absorption solar collector [21]. The influence of particles on the radiative energy absorption has been of interest for long time for many applications. Recently researchers have become attentive in the radiative characteristics in liquid suspensions for many applications [22,23] because of the capability of the absorption spectrum [24] and the large potential enhancement to the effective optical characteristic of the system [21].

1.2.1. Solar collector classification

An apparatus known as a solar collector gathers solar radiation events on it, transfers them into thermal energy, and thereafter conveys this energy to a working fluid (air or water). The thermal energy storage system may be charged with the heat that the working fluid absorbs and utilized at night. For photo voltaic (PV) utilization PV module converts solar radiation into electrical energy. In addition to it, it also produces abundant waste heat, which can be utilized by attaching PV board with recuperating tubes filled with carrier fluids [18,25]. Figure 1.4 clarified several solar collector types. The two main kinds of solar collectors are fixed collectors and tracked collectors. While tracking collectors follow the movement of the sun such that incoming solar radiation constantly incident perpendicular to them, stationary collectors are kept at rest. Single and double axis tracking are the two categories into which tracking solar

collectors are separated. There are three types of fixed collectors compound parabolic, evacuated tube, and flat plate. The three different forms of single axis tracking collectors are parabolic trough collectors, cylindrical trough collectors, and linear Fresnel reflectors. Once more, the central tower receiver, parabolic reflector, and circular Fresnel lens are subcategories of the double axis tracking collector [18].

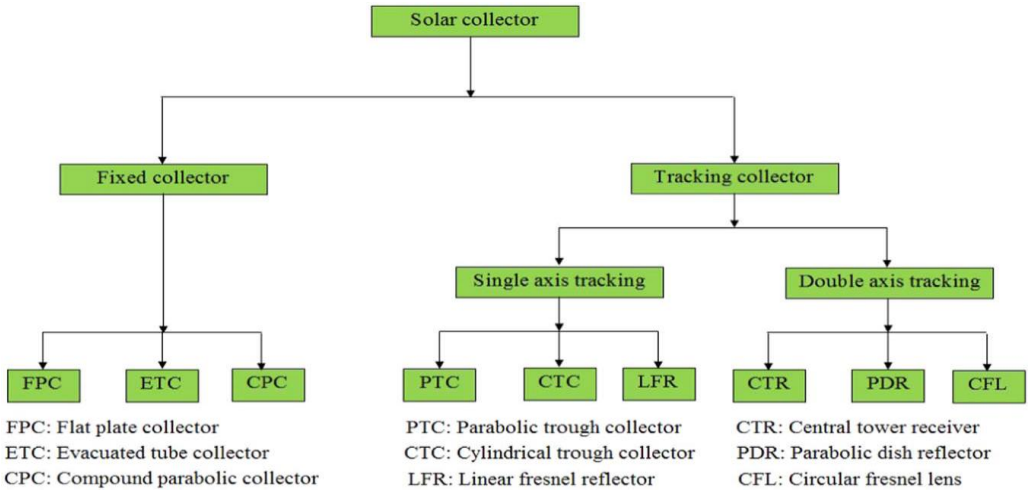

Figure 1.3. Types of solar collector [25].

Accordingly, the kind of heat transfer fluid and the materials used in their construction (pure water, non-freezing liquid, air, or heat transfer fluid), as well as whether they are covered or not, solar thermal collectors may also qualify as legendary. When used for water heating, solar flat plate collectors have an efficiency of over 70%, which is quite high compared to solar direct energy conversion systems, which have an efficiency of about 17% [26]. These collectors are useful for low temperature industrial applications, heating, and domestic applications. Many solar collectors based on concentrating solar power systems are now on the market. Systems employ lenses, mirrors, and tracking systems to concentrate a vast area of sunlight into a narrow beam, which is then used as a heat source for a conventional power plant. The parabolic trough, the concentrating linear Fresnel reflector, the concentrating sterling dish, and the solar power tower collectors are only a few examples of the wide variety of concentrating technologies which have been created. Recently, a novel method of nano-fluid-based solar collectors was developed by combining the solar thermal configuration system with cutting-edge nano-fluid and other nano particle suspension technologies [27].

1.2.2. Solar Collector Techniques

Parabolic trough collectors, linear Fresnel reflectors, power towers (also known as central receiver systems), and dish-engine systems are the four major types of solar collectors, and they produce local temperatures of (550°C, 550°C, >1000°C, and 1200°C), respectively [28].

1.3. HEAT TRANSFER TECHNIQUES

Heat transfer improvement techniques are categorized as active, passive and compound methods [29]. In the active method either of the following techniques are depended to improve the heat transfer:

- Surface rotating process.
- Process of vibration the heat transfer surface.
- Construct a pulse on fluid surface.
- Introducing a magnetic or electrical field to the heat exchanger.
- Injection a fluid in the fluid flow-single phase.
- Elimination of vapour-two phase.

In the passive method no further energy is wasted unlike the active method to improve the rate of heat transfer. In this method the tube surface is either developed or inserts are located inside the tube to scatter the regular flow pattern [30]. According to literatures and researches we can find the flowing types of twisted tapes used in researches.

1.3.1. Single Twisted Tapes

Single twisted tapes are had tape width, tape thickness and tape length. as shown in Figure 1.5 [31].

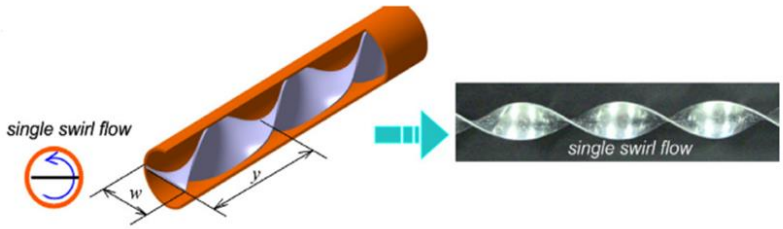

Figure 1.4. Single swirl flow [31].

1.3.2. Twin Twisted Tapes

Twin twisted tapes are had tape width, tape thickness and tape length. Divided into co-twisted tape swirl flow and counter-twisted tape swirl flow as illustrate in Figure 1.6 [31].

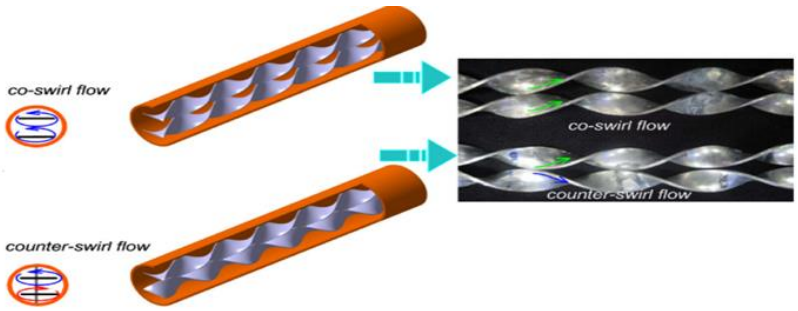

Figure 1.5. Twin co-twisted tapes and twin counter twisted tapes [31].

1.3.3. Porous Disc Receiver

Solid disc at the bottom, porous disc at the top, solid disc at the bottom, and an alternate porous disc are the positions of the porous disc receiver. as shown in Figure 1.7 [32].

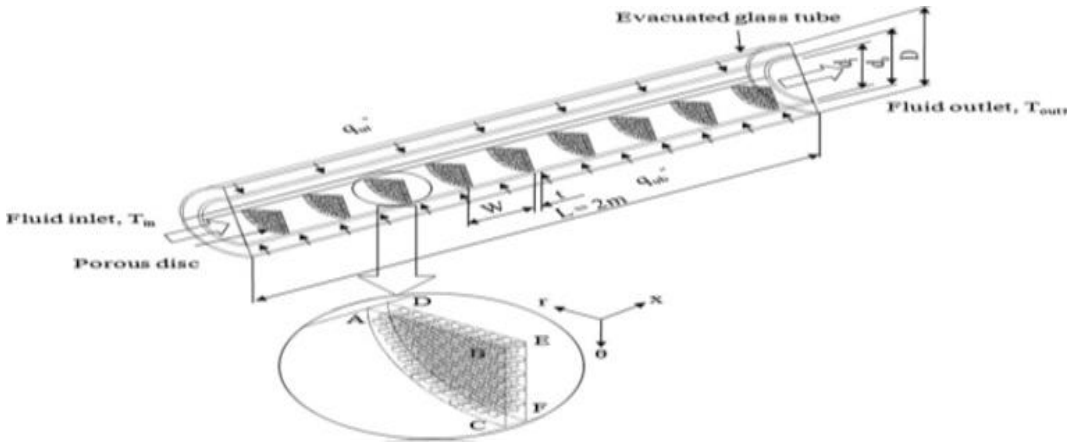

Figure 1.6. Porous disc receiver in section [32].

1.3.4. Geometric Variables of the Helical Fin

Internal helically finned tubes is an internal finned tube with a moderated helix angle and longitudinal fluid swirl, and it closely matches our expectations for our PTC design. as shown in Figure 1.8 [33].

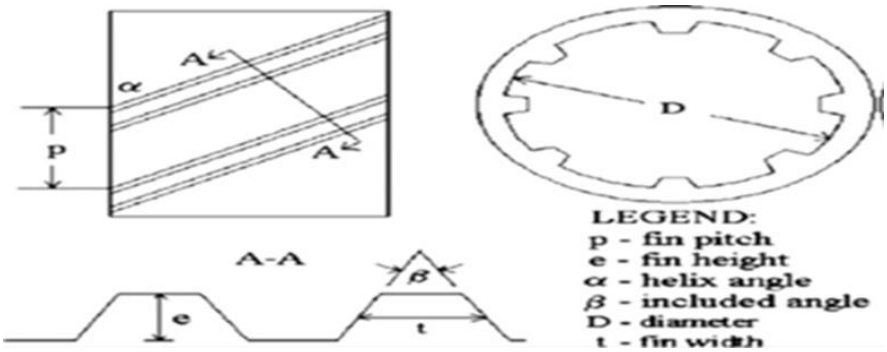

Figure 1.7. Geometric variables for the helical fin [33].

1.3.5. Longitudinal Vortex Generation

Longitudinal vortex generators, are placed on the side of the absorber tube as illustrated in Figure 1.9 [34].

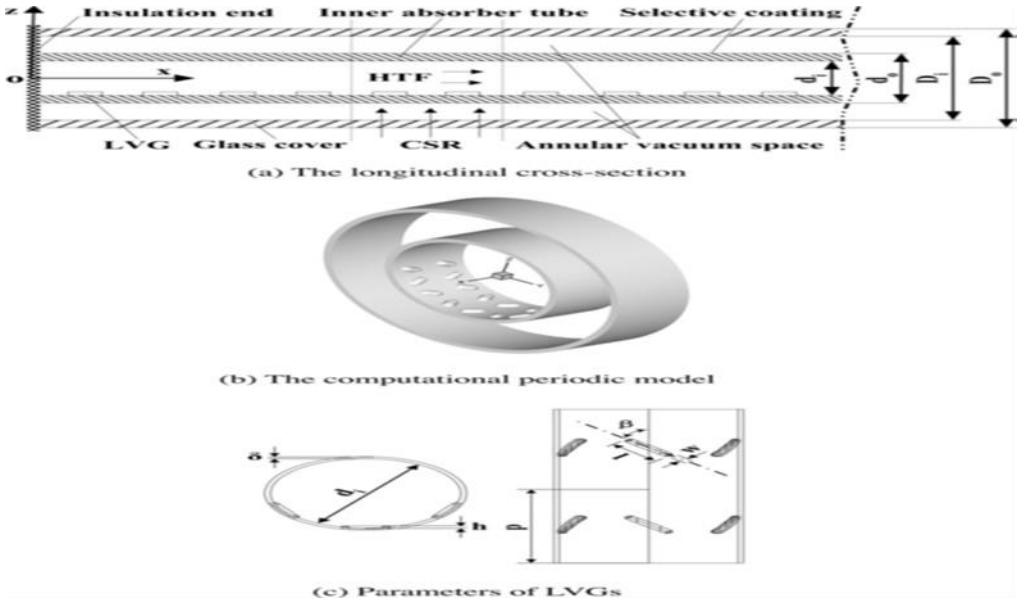

Figure 1.8. Longitudinal vortex generation [34].

1.3.6. Main Types of Considered Receiver Arrangement

Internal multiple fins array, fitted fin into the pipe, as shown in Figure 1.10 reduces a cross section area, in turn increase the fluid velocity, turbulence and the heat transfer coefficient [35].

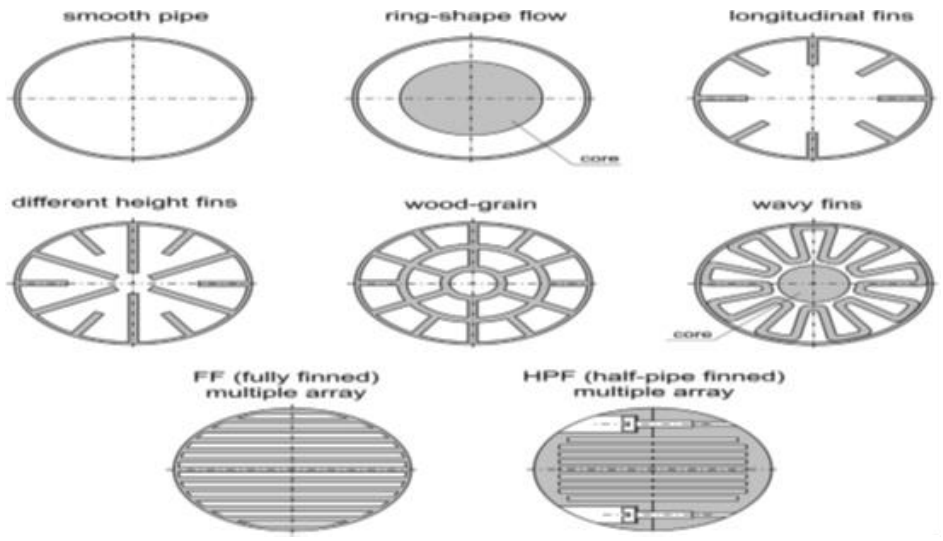

Figure 1.9. Main types of considered receiver arrangement [35].

1.3.7. Louvered Twisted-Tape with Perforations

Louvered twisted tape with perforation, with reducing gap between the edge of a tape, the surface of tube and rising the length of a tape better heat transfer improvement are noted as illustrate in Figure 1.11 [36].

Figure 1.10. Louvered twisted-tape with perforations [36].

1.3.8. Helical-Screw Tape Inserts

Helical-screw tape insert, as in Figure 1.12 [37].

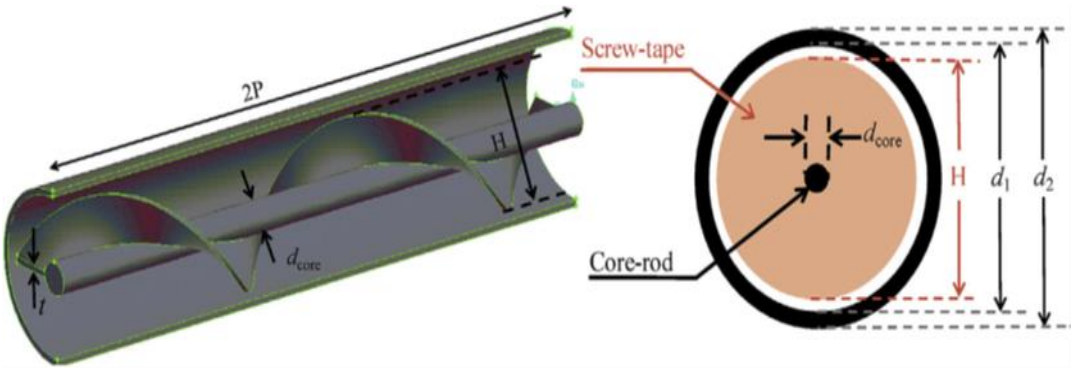

Figure 1.11. Absorber tube with helical-screw tape inserts [37].

1.3.9. Perforated Plate Inserts

The perforated plate, which is set to be propped on a slim axially located rod as shown in Figure 1.13 [38].

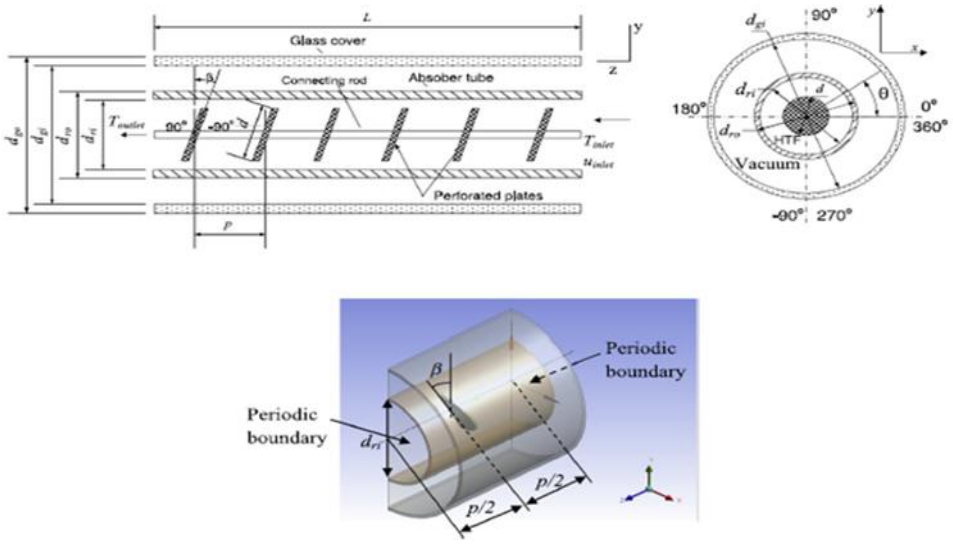

Figure 1.12. Perforated plate inserts [38].

1.3.10. The Dimples Techniques

The dimples as shown in Figure 1.14 with bigger depth, thinner pitch and more number in radial trend are useful at enhancing heat transfer performance improvement [39].

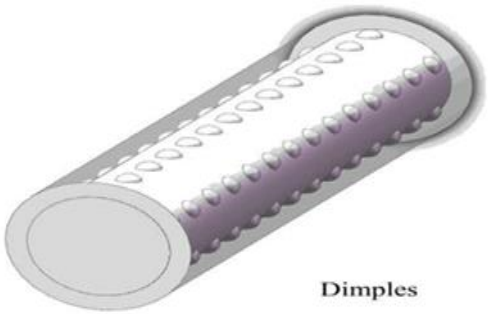

Figure 1.13. The schematic diagram of PTRs with dimples [39].

1.3.11. Converging-Diverging Absorber Tube

As illustrated in Figure 1.15, a converging-diverging absorber tube is constructed with a wavy interior surface to improve heat transfer performance. This also increases flow turbulence, which improves the conditions for heat transmission [40].

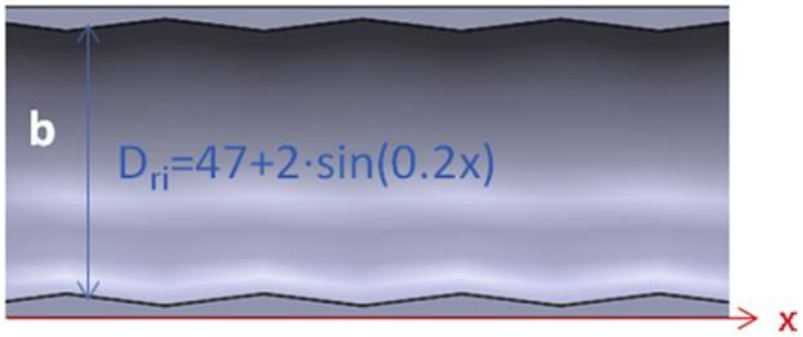

Figure 1.14. Converging-diverging tube [40].

1.3.12. Wavy-Tape Insert

Wavy-tape insert, it considered a swirl flow generator as shown in Figure 1.16 [41].

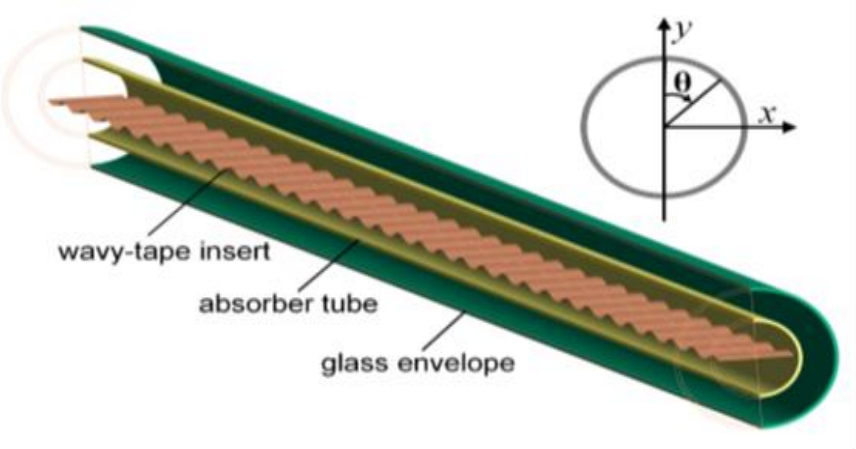

Figure 1.15. Wavy tape insert [41].

1.5.13. Discrete Double Inclined Ribs

Discrete double inclined ribs, which is shown in Figure 1.17 and respected swirl flow method, to increase the turbulent in the flow [42].

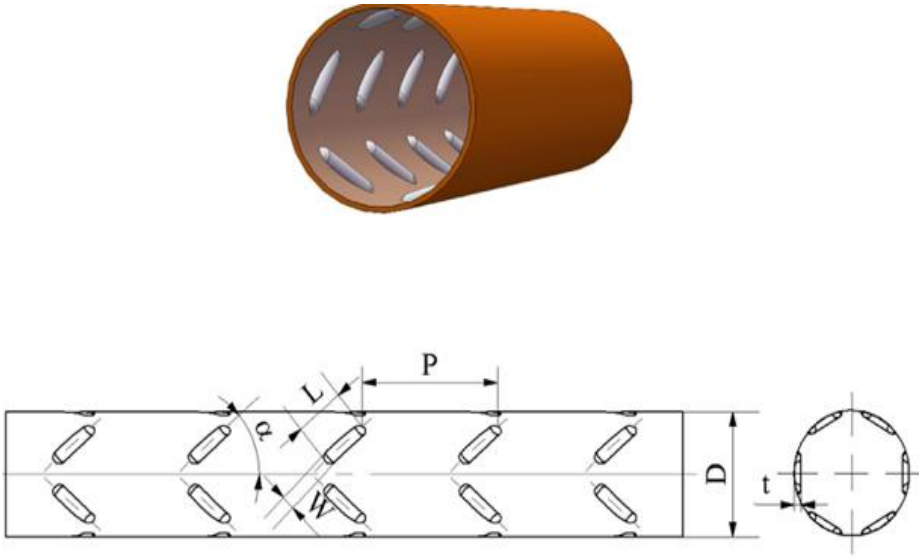

Figure 1.16. Discrete double inclined ribs [42].

1.3.14. Square Perforated Twisted Tape Inserts

Which is shown in Figure 1.18 the multiple square cribriform twist inserts parameters are specified by tape cribriform twist length and width, that expressed as dimensionless roughness [43].

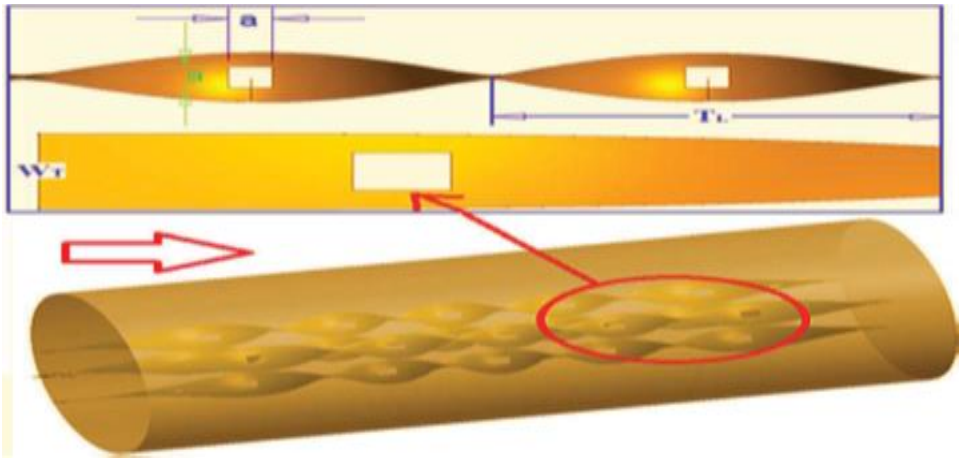

Figure 1.17. Square perforated twisted inserts [43].

1.3.15. The Butterfly Inserts

The butterfly inserts are made from aluminium sheet and consist from a holding rod. Between the butterfly pieces a distance expressed as pitch length. As seen in Figure 1.19 [44].

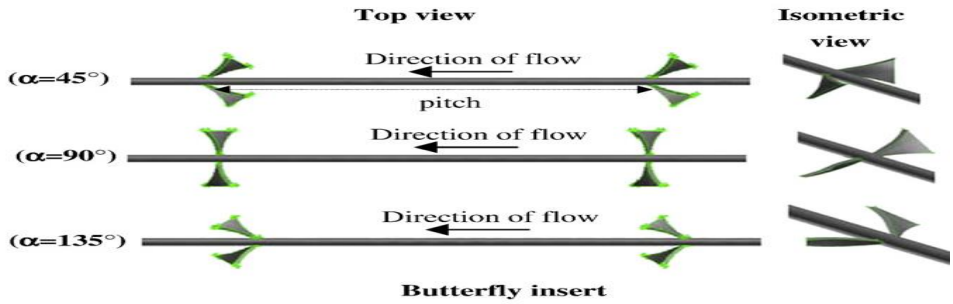

Figure 1.18. Butterfly inserts [44].

1.3.16. Wire Coil Inserted

coil wire of inserted, parameters as seen Figure 1.20 are the helical pitch, the wire diameter and the inner pipe diameter [45].

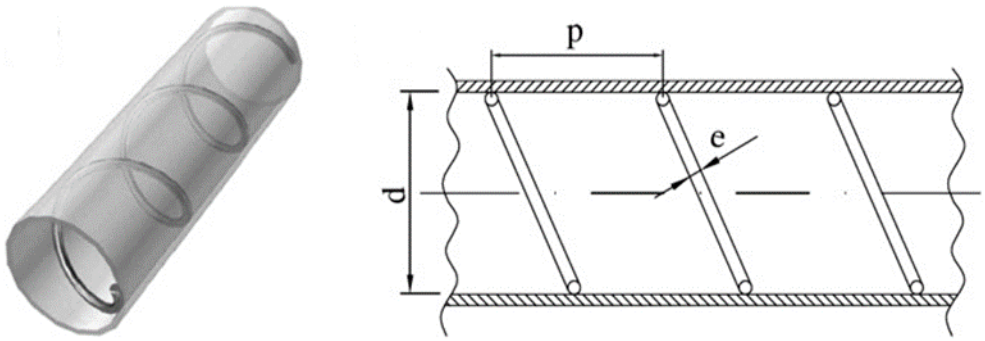

Figure 1.19. Wire coil inserted [45].

1.3.17. The Conical Injector Type Vortex Generator

Conical injector type vortex generator, Figure 1.21 an illustrates the conical injector type vortex generator geometry, which is fricated of galvanized sheet with different

angles. The flow directors are attached to every hole at three different angles to radial direction as seen in Figure 1.21.b [46].

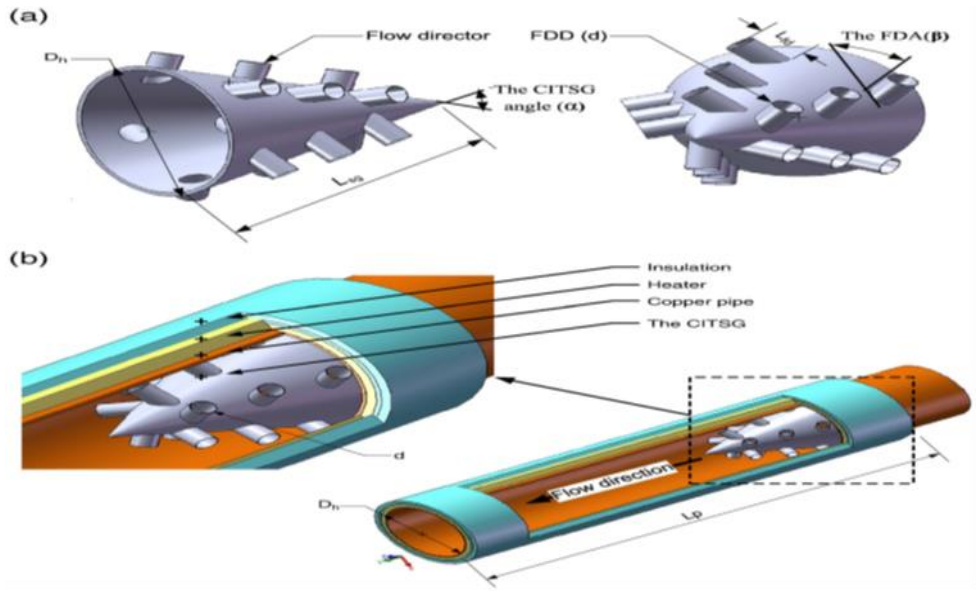

Figure 1.20. (a) detailed figure of conical injector type vortex generator, (b) the conical injector vortex generator for flow pipe [46].

In this study we used single twisted tape inserted in side tube of copper material to heat pure water, fixed in parabolic solar collector, in different cases. The heat flux was constant.

1.4. COMPUTATIONAL FLUID DYNAMIC

Solar collectors' different categories according to operation temperature. Non-glazed panels, flat plate composes piece of low temperature solar collectors and evacuated tube collector, line centring and point centring collectors composes the high temperature solar collectors' category. To decreasing the cost and time for research and development, techniques as computational fluid dynamic can be utilized to simulate solar water heating system by supplying hypothetical conditions which can produce close to realistic results. By applying computational fluid dynamic simulation models, the cost of installation and maintenance can be neglected which is a main obstruction in experimentation. Simulation analysis not conserve the cost and the time only but also gives in depth analysis, which is not possible through experimentation,

for example applying computational fluid dynamic simulation could estimate the distribution of temperature inside the equipment [47]. Computational fluid dynamics simulation aids for calculating the system optimum design also, and then analysed the complex energy systems. As well as, studied the system under different conditions of weather, that otherwise extremely time consuming [48]. CFD, is regarded a validating numerical method that can model separated particles by following each motion of particle in the flow, as well as it is capable for simulation the complicated fluid flows with a quantitative and qualitative characterization of the spatial and temporal the flow field changing [49]. In practice, the matters particulate is introduced to the aerodynamic systems with gases flow, in turn it could be considered as multiphase flow. Therefore, computational fluid dynamics models are mainly utilized to hold the air or fluid flow properties successfully with fundamental data in estimation the behaviour of aerodynamic [50–53]. The governing equations, such as those relating to mass, momentum, energy, etc., are determined and solved for the several cells in the computational fluid dynamic. There are several computational fluid dynamic tools available, including the finite volume technique [54–56] and the finite difference method have been already utilized for simulation flow modelling [57]. The computational fluid dynamic approach's repute has already been supported by research. Additionally, no research has been done to determine how to optimize this method for computations. The use of artificial intelligence algorithms might improve the computational fluid dynamic techniques in terms of methodology. In the most recent years, artificial intelligence algorithms have performed important roles in the optimization of the computational fluid dynamic technique and the reduction of numerical simulations [58]. The numerical calculations are performed applying the computational fluid dynamic code in ANSYS FLUENT platform, available for the regarding geometries. For each cell, the main equations are solved for pressure, temperature, and structure flow. Making the 3D geometrical model of the case study with the drawing module of the computational fluid dynamic software is the first stage. The second stage contains the generating of mesh [58].

1.5. TWISTED TAPE INSERTED TECHNIQUE

Utilizing of twisted tape fitted on the flow consider the most common techniques [59]. The twisted tape inserted applications of ducted heat exchangers, as a passive method to enhance heat transfer, were largely investigated. Several twisted tapes designs were applied in several equipment for heat transfer increasing [60–62]. Practically, the using of twisted tapes perform an important base to enhance the heating systems of solar water performance of [63], since twisted tapes may inserted in the solar water heating systems flow tubes to improve the rate of heat transfer, in other hands the power of pumping may rise considerably, in turns its cost becomes considerably through the operation [59]. The vast application and concern in utilizing twisted tape for the turbulent and the laminar flow can be observed in several dedicated studies for improving of heat transfer utilizing twisted tape inserts available in reviews. Additionally, a great deal of twisted tape insert changes has been detecting. These include twisted tape inserts with regular spacing, short length twisted tape inserts, twisted tapes with cuts, twisted tapes set apart from the wall, and twisted tapes with wire nails etc, [64]. Twisted tapes became preferable tools for heat transfer improvement in the heat exchangers as their low costs and easy installation. Heat exchangers thermal performance improves highly in the existence of twisted tapes inserts [65]. Twisted tapes augment swirl strength and perturbation of the fluid in the tubes of heat exchanger, in turn causes to an augment in rate of the heat transfer and pressure drop inside tubes improved by twisted tapes. Several different modified twisted tapes were studied in the past little years and mostly all of the numerical and experimental studied confirm that the thermal performance is hardly depending on the twisted tapes shapes [66–70]. Friction factor on twisted tape inserts is highly less than that in a smooth tube according experimental investigations on regularly spaced twisted tape elements in a circular tube [71]. Heat transmission is increased as the twist ratio declines [72]. Twisted tapes insertion in the tube supplies a simple passive technique improving heat transfer convective by creating swirls in the flow by obstructing the boundary layer at the wall of tube because of iterative changes in the geometry surface [73]. By focusing on the pitch and width ratios effectuates [59]. Using the twisted tape inserts in tube for parabolic collector, there is indication, that the higher collector thermal performance twisted ratios that are low working at low

values of Re. This kind of collector attached with wall separated twisted tape inserts [38]. An increasing of twist ratio and reduction of width ratio, the perfect Re improved [74]. The enhancement of pitch ratio leads to an augmenting in friction factor, Nu, and overall thermal performance [75]. Twisted tapes may not be the best insert tools and their wide-scale utilizing is attributed to the correlations lack for other insert tools [76].

PART 2

LITERATURE REVIEW

Hamzah et al. studied the effect of twisted tape ratio on a swirl effect inside a long half-length pipe. They showed that the simulation of flow set at different range of Re various twisted tape ratio, average outlet temperature, Nu, and heat transfer coefficient, power losses were compared with plain pipe. Results showed that, the swirl geometry would be effect by 10% [76].

Nakhchi et al. designed numerical simulations, used Response surface method to study the performance of fitting tubes has cross-cut twisted tape with alternative axis at turbulent flow thermal. The results showed that thermal performance improve with increasing cross-cut ratio of the twisted tape's width [77].

Venkatesan et al. conducted an experiment with a double-glazed V-trough solar collector fitted with plain twisted tape, as well as twisted tape with a vertical and horizontal wing fitted for two different twist ratios. The results indicated that the observed double - V trough heat transfer capacity is best than an single glass V-trough sun collector by 8.84%, hence the reduce heat loss coefficient and enhanced the performance of heat transfer in double glazing glass collectors [78].

Arjmandi et al numerical simulation model to investigate the effect of applying the new vortex generator combined turbulent twisted tape and specified Nano-fluid as working fluid. The outcomes showed that the pitch ratio caused an increase of efficiency up to five times as compared to original case. Additionally, Nu were increased, when the angle of the vortex generators in the new combined turbulent decreased [79].

Amani et al. performed numerical simulation model to investigate the influence of the impact conical strip insert on the parabolic trough collector thermal performance, for that purpose finite volume method was proposed. The results proved that Nu was increased up 91.94%. And friction factor was (5.31) greater than the empty tube. The gross thermal hydraulic performance of parabolic trough collector thermal was varied from (1.107 - 0.679) [80].

Afsharpanah et al. presented simulation model by using different kinds of modulated multiple twisted tape inserted in solar PTC to increasing heat transfer performed by ANSYS FLUENT CFD. Showed that the average Nu of case at dual v-cut twisted tapes were more than plain tube about (17.44%-19.58%), the thermal performance of all cases with various twisted tapes and dual square-cut twisted tapes was the best case compared with plain tube by (12%-16%) enhancement. The lowest thermal performance was Perforated dual twisted tape [81].

Al-Obaidi et al. created simulation model by using CFD methods to verify a numerical calculation of flow in the pipe of heat exchanger with variation of wall extension. The numerical results indicate that flow and heat performance had been more influence by the change of twisted tape. In the results twisted configurations can increase friction factor about (5.4% - 33.5%). Thermal evaluation factor was greater than 1.66 [82].

Arasteh et al presented simulation model to evaluate a heat transfer improvement by inserting rotating or stationary twisted tape inserts. The results showed that an increasing the twisted tape inside a tube to increase the consumption energy, heat transfer. In case of stationary condition, decreasing of pitch distance result in higher Nu simultaneously with more friction factor. Twisted tape began to rotate, friction factor and Nu were extreme increased. The decreasing of the pitch distance recorded a peripheral effect on the friction factor and Nu. Additional increase in the angular velocity enhanced the average Nu, but expend of much more friction factor and consumption of energy [83].

Azizi et al. studied the effect combination of twisted tape pipe, as passive method, and injection of air, as active method, on increasing of heat transfer. A horizontal tube was

counted as test section under applying heat flux was constant. Maximum increment for the Nu and pressure loss due to the decrement of twisted pitch about (35% & 81%), respectively [84].

Dandoutiya et al. investigated a double pipe heat exchanger employing thermal performance cut-twisted tape. Showed that the influence of twisted tape leads to swirl flow in two zones nearby the wall of tube, the wall of twisted tape. Nu enhanced but friction factor augmented as compared to empty tubes The more value of thermal performance factor equal to 1.21 was noted Re (5500) [85].

Kumar et al. carried out numerical simulation model, and introduced a new triangular perforated twisted tape with V- cut. Were showed that at lower pitch the best thermal hydraulic performance investigated. The thermal performance factor value more than empty twist tape insert by 1.49 [86].

Rawani et al. developed C++ analytical mathematical model twisted tape insert for PTC, to evaluate rise of temperature of fluid for estimation of performance at certain condition. Results showed that at twisted ratio equal to (1), Nu divided by heat transfer coefficient at mass flow rate was over plain absorber of parabolic trough collector, and corresponding improvement in thermal efficiency. [87].

Bellos et al. Investigated some common thermal improvement techniques for enhancing the performance of non-evacuated and evacuated of PTC. Employing of twisted tape inserts, inserts finned absorbers, and cribriform plate inserts, were compared with the reference case of the absorber. According to results, thermal efficiency enhancement for evacuated and non-evacuated tube collector. The twisted tape inserts and perforated plate inserts were gave lower improvement , for the non-evacuated collector [88].

Hayat et al. introduced a new twisted tape with trapezoidal ribs and performed CFD simulation model the proposed insert made swirl motion and raised the intensity of turbulence in flow of fluid. Showed that increased rate of heat transfer in twisted tape

with trapezoidal ribs duo to higher intensively of turbulent, which Caused by ribs trapezoidal [89].

Ju et al. investigated three dimension numerically model to examine Multiple semi-twisted tape inserts hydrothermal performance The results referred that, when the number of semi-twisted tapes and swirl flow streams increased, which caused to an enhancement in the local Nu in addition to the friction factor, The increase in concentration of Nano-fluid improved the average Nu and friction factor [90].

Raheem et al. investigated Computational Fluid Dynamic model for PTC with helical screw tape insert in the tube to study the efficiency of the system. The results parametric investigation was showed that pressure drop and Nu were increased with increasing of thickness and helix angle, but Nu trend to decrease with increasing the inner diameter. The modified by inserts, with fins or holes in the inserts produced an increasing in pressure with a little increasing in Nu. The tapered helix design was reduced pressure drop by 12% but decreased Nu 5% [91].

Saedodin et al carried out numerical simulations in three dimensions to examine fluid flow and heat transfer in a solar PTC consisting helical profile along the pipe on wall of collector, by proposing finite volume method, which was utilized from CFD code. Showed that at inlet velocity (0.3 m/s) thermal efficiencies with (2-6) of elements more than parabolic trough collector by 6.6%, 13.2%, 20.6% and 27.6%, respectively. Results showed that maximum thermal efficiency at cross-section, enhancement by 29% [92].

Thakur et al. presented an overview on numerical based studies CFD for various types of methods which were used for efficiency enhancement of flat plate solar collectors. Nano-fluid using, PCM and polymer, changing the design of absorber plate and using of inserts and reflector for climbing performance of flat plate solar collectors were discussed. The twisted tapes inserts increased the heat transfer [93].

Kundan et al. investigated experimental study a horizontal double-tube counter-flow heat exchanger with twisted tape inserts and empty tube. Different twist ratio and TiO_2-

H_2O nano-fluid were applied. Revealed that the heat transfer coefficients were increased directly with volume concertation of TiO_2 nanoparticles. The simulated specific that no considerable effect on the heat transfer coefficient values at 0.05% volume concentration when size of TiO2 nanoparticles of TiO_2-H_2O equal (30 mm and 50 mm) [94].

Mashayekhi et al. investigated simulation model for stationary and rotating of twisted tape inserts in equipped tube, Al_2O_3 water nano-fluids was used. The results clarified that a twisted tape essentially increases heat transfer coefficient as compared to the empty tube. the rotating twisted tape as compared with the stationary twisted tape indicates a significant capable to enhance the average Nu relating with the angular velocity. The improvement in the average Nu was increased in fixed and decreased in rotating conditions when comparing with empty pipe [95].

Sarviya et al. achieved experimental research of a new type of twisted tape inserts have continuous cut edges. analysis of heat transfers, an experiment's findings showed that using twisted tape inserts with continuously cut edges might increase heat transfer rates while maintaining a manageable pressure drop [96].

Rezaei et al. investigated numerical simulation of microchannel with a triangular section (ribs), fluid water employed as the base flow the effect of volume friction of nanoparticles on the heat transfer and flow physics, which considerable turbulent flow, were studied. Indicate that, ribs have influence on the flow physics, and their effect is defiantly to Re. heat transfer increases, while, more pressure drop generates [97].

Yang et al. carried out steady state numerical simulations of a tube and shell heat exchanger with twist tapes inserted. Heat exchanger thermal hydraulic performance with deferments twisted tape width and twist ratios was performed. It was made clear that the combined impact of the geometric and structural improvements improved the design's performance [98].

Eiamsa-ard et al did an experimental investigation on a micro-fin tube using a combination of approaches, swirls created by twisted tape, and nan-fluids. The

experimental findings showed that as twist ratios for non-uniform twisted tapes were lowered and Nano-fluid concentrations were raised, heat transmission, friction loss, and thermal performance factors were increased. And compared to co-current arrangements, counter-current arrangements improved heat transmission more [60].

Jaramillo et al. developed an experimental model of the performance of PTC by inserting a twisted tape The experiment results that (friction factor, Nu, and thermal efficiency) increased as compared with decay tube, when the twist ratio and the Re were decreased. These quantities didn't provide an improvement when the twist ratio were increased. Twisted tape inserts improve thermal fluid and the heat transfer by creating a swirling flow, but increased too [59].

Kumar et al. investigated using an insert made of twisted tape for a solar water heater, heat transfers in the twisted tape insert collectors were increased as compared to plane collectors. Thermal performance was increased by 30% in the plane solar. The twist ratio was developed in the form of ($^{Nu_s}/_{Nu} = 1.3 + \frac{2.88}{y}$) the twisted-tape collectors work better in low Re [99].

Hobbi et al studied how a flat-plate solar collector's thermal performance was affected by heat enhancement devices. The investigation showed that the applied methods were ineffective in increasing transmission of heat to the collecting fluid [100].

Jaisankar et al. presented and performed helical twisted tape equipped with various twist ratios thermos-syphon solar water heater, which induces swirl flow in the tube in turn increases heat transfer, the results showed that heat transfer enhancement with twisted tape fitted was higher than the plain tube collector at minimum twist ratio and decreased gradually with increased twisted ratio. With increasing sun intensity, the twisted tape collector's total thermal performance rose [101].

Sekhar et al performed convective heat transfer analysis for a horizontal circular tube range utilizing experimental simulation at constant heat flux boundary condition. The variation of heat transfer coefficient in the flow of pipe for Nano-fluids and water with

twisted tapes were analysed. The particle concentration dependence and Re for enhancing in heat transfer and rise in the power of pump [102].

Sandhu et al. presented an experimental investigation using wire coil inserts, wire mesh inserts, twisted-tape inserts, and insert devices to explore the flat-plate solar collector's thermal efficiency, at specified range of P_r and Re utilizing water. The results were indicated the improvement of the Nu. Comparing the best inserts revealed that under the regime of laminar flow, the best performance at mesh insert while, the concentric coils performed the high Nu increase in the turbulence regime, as compared to the smooth pipe. Concentric coils were the best insert among those tested [70].

Chang et al. investigated a numerical study using FLUENT code to investigate the twisted tapes' improved heat transmission in a molten salt solar receiver tube. The results revealed that twisted tape inserts could considerably improve the temperature distribution on the tube surface [103].

Ghadirijafarbeigloo et al. developed 3D numerical simulation using an experimental laboratory trough collector included absorber tubes with various tape inserts. To improve heat transfer by generating turbulent swirling flow. Showed that the heat transfer coefficient increased considerably where comparted to a plain tube [36].

Syed et al. presented an experimental investigation for studying the effect of absorber device nail-twisted tape inserts of a solar PTC using nano-fluid as the working fluid. Indicated an improvement in the heat transfer performance of the solar trough collector, and increasing nano-fluid viscosity was created by swirl flow, increasing particle volume concentration, and increasing friction factor with twisted tape absorber [104].

Syed et al. presented an experimental investigation of absorber tube twisted tape inserts in solar parabolic trough collector to get optimum process parameters. The results indicated significant increase augmentation in Nu in addition to friction factor could be obtained at elevated Re [105].

Eiamsa-ard et ala helical tape was inserted in the tube to create swirling, which increases heat transmission in the tube, according to an experimental investigation. The use of helical tapes caused a greater rate of heat transmission than utilizing a simple tube, according to experimental findings. The full-length helical tape with rod contributes the greatest rate of heat transmission and performs superior to that without rod [106].

Chin et al. studied the effects of the number of perforations and the perforation diameter on each pin, and employed limped perforated pin fins to increase the rate of heat transmission in these devices. The findings showed that the perforated pins had a greater Nu than the traditional solid pins [107].

Durga Prasad et al experimentally investigate a U-tube heat exchanger with twisted tape insert, to improve the heat transfer rate of Al2O3 Nano-fluid as working fluid. An experimental results indicated enhancing in Nu about 31.28% at specified flow rate, Re for concentrations of nano-fluid as compared with water, but the friction factor was increased as compared with water [108].

Guo et al. proposed a centre-cleared twisted tape to achieving thermos-hydraulic performance, and performed numerical comparison study between it and the short-width twisted tape. The numerical results established that the resistance flow could be decrease in both methods, but different in thermal behaviours from each other. Heat transfer enhanced by (7%-20%) at twisted tapes, with a central clearance ratio as compared with normal twisted tape [109].

Salman et al. carried out CFD simulation model of copper-water nano-fluid flow at constant heat fluxed tube with presence a new arrangement of vortex generator. Indicated that the improvement of the heat transfer rate produced by the typical and Parabolic-cut inserts augmented with twist ratio and cut depth reduced. Heat transfer improvement increased directly with the volume friction of the CuO Nano-particle. Additionally, the twisted tape improvement of the average Nu with considerable increasing in friction factor than at typical twisted tape [110].

Yadav et al. performed CFD simulation model of air flow inside an annular tube with a partially empty and partly swirl flow in Four configurations. The simulation resulted that, the heat transfer coefficient and the pressure drop in the full-length twisted tape greater than those in the of the plain tubes case without inserts [111].

El-Said et al. were presented a novel plate heat exchanger applied helical flow duct in a series configuration in counter flow of water as working fluid, pitch ratios and variation flow channel cross section part ratio were analysed for different Re. The results showed that considerable increased in friction factor with than other pitch ratios [112].

Bhuyan et al. performed a simulation study of a tubular U-loop pipe, an improvement of heat transfer at empty, with twisted tape inserts was investigated. The simulations were regarded for the stationary and periodic at different length of inserts. The results showed that with the increase of the length of inserts, the heat transfer considerably improved [113].

Piriyarungroj et al carried out numerical simulation to estimate turbulent flow in a circular tube provided with loose-fit twisted tapes. Indicated that in spite of increasing of Re, the reduction of the clearance ratio produced an increasing in the pressure loss and. heat transfer [114].

Sharifiet al. investigated CFD simulation study for double pipe heat-exchangers. The effect of coiled wire inserts on the Nu, efficiency and friction coefficient in double pipe heat-exchangers was employed. The results indicated that wire coils may enhance Nu data about (1.77) times [115].

Al-Obaidi et al performed numerical simulation model of heat exchanger circular pipe with twisted tape inserted. Simulation results showed that using twisted tape inserts in pipes could produce considerable increasing in flow resistance caused an increasing in pressure difference. And temperature difference indicated an increasing directly with numbers of twisted tape inserts as compared with temperature difference in the empty for tube [116].

Chu et al. carried out a comparative investigation on flow pattern with various twisted tapes using CFD. Result verified that the Nu and friction factor were augmented, when the space is decreased thermal performance was enhanced. Introducing fluid into the cut region in V-cut toward wall of the tube produced heat transfer increasing closed to the tube wall. Comprehensive thermal performance of windward V-cut twisted tape as compared to the isosceles V-cut was increased from (1.15 to 1.18) to (1.16 to 1.21) [117].

Akram et al. studied the clove-treated graphene Nano platelet Nano fluids effects on the performance of flat-plate solar collector. Verified that thermal performance of solar collector improved with increasing concentration of mass and mass flow rates and reduced with a rise in reduced temperature parameter [118].

Damarlal et al. reviewed the experimental study for evacuated tube solar water heaters with twisted inserted tape. The experimental results reviled that at high flow rate, the earning in temperature was low as a result of less time for retention of water. Short pitch twisted tape generate more turbulence as compared to the long pitch twisted tape, which produced more increasing in water temperature. Additionally twisted tape with short pitch given better thermal performance than others [119].

Habeeb et al reviewed the experimental and numerical studies by using a circular tube with different shapes inserted. In comparison to the standard twisted tape, the twisted tapes with a centre wing and alternate axes could generate the maximum heat transfer improvement coefficient. Twisted tape with constant pitch, works better than gradually decreasing length tape [73].

Tusar et al investigated simulation model for turbulent flow through tube with inserted twisted tape results gave that when twist ratio of (3.46) and (7.6), where Nu and friction factors were augmented, and thermal performance factor ranged (0.9 - 1.2). Twisted tapes improved heat transfer more effectively at comparatively lower Re [120].

Alzahrani et al. prepared CFD simulation model, for investigating thermo-hydraulic properties of forced and natural water convection at different arrangements of twisted

tape inserted in tube. The simulation showed that an improvement in heat transfer and increasing in pressure drop. Twisted tapes along sub-channel for the water flow were showed enhancement in Nu and rising in pressure drop when compared to the arrangement of plain sub-channel [121].

Karanth et al. investigated experimental and numerical study for sinusoidal flow passage, which increased turbulence, consequently increased heat transfer convection. The experimental and numerical analysis revealed the straight tube arrangement had better performance as in sinusoidal pipe arrangement [122].

Yao et al. constructed a numerical model for collector tube with twisted tape inserted to analyse flow transfer and fluid. Numerical results indicated that, the twist tape inserts decreases velocity and produce uniform field of the temperature. At relatively high temperature the twist tape inserts assist heat transfer, while at relatively low temperature not conductive to heat transfer. The mean Nu of the solar water heaters greater than the typical solar water heater [123].

Jasim et al. prepared experimental and numerical investigation of inserting a closed tube inside the riser pipe. And find the impact of working fluid amount on the thermal performance. As numerical results demonstrated a noticeable influence on the thermal performance with amount of working fluid through the thermos-syphon loop. As well as, a correlation equation to estimate water temperature inside the storage tank has been achieved with thoroughness about 95.6% [124].

Keen et al. developed experimental study of twisted tape inserted in evacuated tube solar water heater. Experimental showed that heat transfer and outlet temperature of working fluid in the twisted tape inserts, more than at evacuated tube without twisted tape [125].

Reddy et al. achieved numerical and experimental investigation of PTC, nano-fluid was used as working fluid. Indicated Nu and friction factor were insignificantly more with maximum improvement efficiency ratio of (0.845) for twisted tape insert as compared with plain tube. An enhancement of average Nu for twisted tape inserts was

41% with plain tube. likewise, friction factor for tube with twisted tape insert was 32% as compared with plain tube [126].

Sunil Yadav et al. developed numerical investigation of collector with twisted tape, to enhance performance without increasing of contact area nor increased of pressure drop. This was attended by converting velocity head to presser head the loss as the diameter was expanding gradually. In turn increasing heat transfer efficiency without any increment in pressure loss [127].

Xue et al proposed numerical analysis of three novel wavy plate fin types and the plate fin heat exchanger. There are three types of wavy fins: staggered, perforated, and discontinuous. When compared to conventional wavy fins, the simulation results showed that the swirl flow and effective fluid mixing, the perforation, serration, and breaking arrangement were beneficial for enhancing heat transfer [128].

Dehankar et al. highlighted the effect of passive techniques such as, rectangular holes, circular holes, wavy rate, tape size and angle of entry on the optimum thermal enhancement factor. Friction factor and heat transfer rate and enhanced by 25% as applied full length tapes when compared on a blank tube, and Nu increased (9) times. There was increasing applying different twisted tapes [129].

Ghalambaz et al. prepared numerical simulation model of heat exchanger with twisted tape elements to inspect influence of pitch value, twisted tape cutting percent, location and Re. The simulation indicated fitting twisted tape and decreasing the pitch value considerably increase Nu, friction factor and performance when compare with the empty tube. An augmenting the twisted tape cutting percent decreases pressure drop and heat transfer [130].

Yılmaz et al. developed parabolic trough solar collector with triangular cross section wire coil inserted to enhance the performance. The study performed at various wire coil pitches and width and at specified working fluid properties. The results showed that wire coil recorded significant enhancement in performance, and decreasing in the

temperatures of absorber tube. The performance of heat transfer was augmenting more than 183% while the thermal efficiency enhanced between (0.4%-1.4%) [131].

PART 3

THEORETICAL BACKGROUND

3.1. SOLAR RADIATION

The radiation that emits from the sun under the ultraviolet, visible, and infrared zones is significant to applications of solar energy. The wavelength radiation that is significant to solar energy utilizing is between (3.0 -0.15) μm. The wavelengths at the visible zone located between (0.72-0.38) μm. The temperature characteristics of the emissive surface are entirely dependent on the thermal radiation, which is regarded a kind of energy emission and transmission without the need of a carrier in between like in the other types of heat transmission. This speed is determined by the thermal radiation's frequency and wavelength equation [132].

$$C = \lambda * \nu \tag{3.1}$$

Falling the thermal radiation on the body surface, caused reflected portion of it from the surface reflectivity (ρ), absorbing part by the body absorptivity, (α), and transmitting part over the body transmissivity (τ), related in the following equation [132].

$$\rho + \alpha + \tau = 1 \tag{3.2}$$

Should be referred that the radiation characteristics specified not just functions of the surface but also the radiation of incident wavelength and direction. Therefore, Eq. (3.2) valid for the average characteristics through the whole wavelength. Next equation applies for expressing the dependence of these characteristics on the wavelength, (ρ_λ), (α_λ), (τ_λ), spectral reflectivity, spectral absorptivity, and spectral transmissivity respectively related in the following equation [133].

$$\rho_\lambda + \alpha_\lambda + \tau_\lambda = 1 \tag{3.3}$$

Since the majority of solid objects are opaque, $\tau = 0$ and $\rho + \alpha = 1$ are true a body is said to as a blackbody if it completely absorbs all incident thermal radiation such that $\tau = 0$, $\rho = 0$, and $\alpha = 1$ disregard the spectral characteristics or directional preferences of the incident radiation. This is an idealized assumption that does not hold true in practice. A blackbody is both a perfect absorber and has a maximum limit on the amount of thermal radiation it may release. A blackbody's energy emission depends on its temperature and is not evenly distributed across all wavelengths. The monochromatic emissive power is the rate of energy emission per unit area at a certain wavelength. The monochromatic emissive power of a blackbody in terms of temperature and wavelength was first derived functionally by Max Planck. This was done by using the quantum theory, and the equation, called Planck's equation for blackbody radiation, is given by [132].

$$E_{b\lambda} = \frac{C_1}{\lambda^5\left(e^{C_2/\lambda T}-1\right)} \tag{3.4}$$

Where:

$\mathrm{E_{b\lambda}} = \text{Blackbody's monochromatic emissive power } (\mathrm{W/m^2})\ \mu\mathrm{m}$
$\mathrm{T} = \text{temperature of the surface (K)}$
$C_1 = constant = 3.70 \times 10^8\ W.\mu m^4/m^2$
$C_2 = constant = 1.44 \times 10^4\ \mu m \cdot K$

3.2. THERMODYNAMIC MODEL FRAMEWORK

A passive to increase heat transfer in the solar collector tube receiver is method by applying a twisted tape inserts caused the flow rotates axially and changing Re and Nu [31]. A framework for a thermodynamic model is design for determining the solar collector behaviour, when a twisted tape insert is used and the decay tube is taken into account. In order to assess the pressure drop and heat transfer rate under fully matured conditions, the theoretical framework relies on empirical correlations. The framework

for a thermodynamic model is designed for investigating low temperature solar collector regarding that the temperature range between of (70°C-110°C) without changing active fluid [59].

3.2.1 The Solar Collector Modelling

Modelling the solar collector depended on the first law thermodynamic, applying the first law of thermodynamics, the thermal efficiency of the collector is computed. A twisted tape inserts is located to improve convection coefficient in the solar collector receiver tube. The model depends the empirical correlations in [31]. As illustrate in Figure 3.1. The thermal calculations for low temperature solar collector with a twisted tape insert is extremely similarity to the flat plate collector calculations performed. Actually heating Q_u, a concentrate solar collector is related on the conceptual energy balance equation obtained by [132].

$$Q_u = A_a G_B - (1-\eta_o) A_a G_B - A_r h_v (T_r - T_a) - A_r \varepsilon \sigma (T_r^4 - T_a^4) \tag{3.5}$$

Where, T_r in Eq. (3.5), is replaceable the fluid temperature as tube's inlet T_{in} through applying heat removal factor [132], therefore the Eq. (3.5) becomes [132].

$$\dot{Q}_u = F_R\left(\eta_a A_a G_B - A_r U_L (T_{in} - T_a)\right) \tag{3.6}$$

Observe that Eq. (3.6) is a second order equation for focus solar collectors, at low temperature ranges second order term is regardless and approximated with a linear equation.

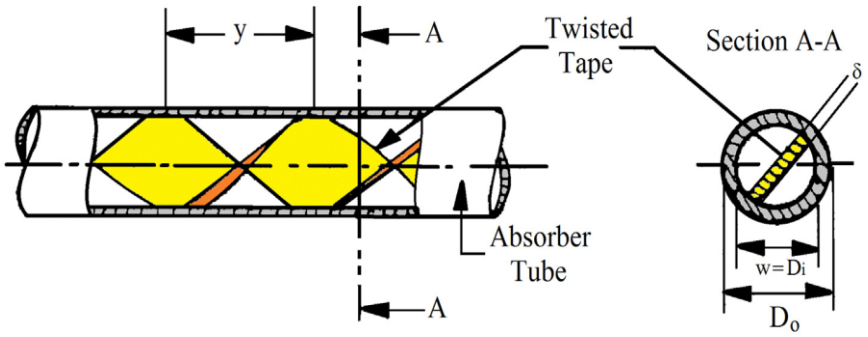

Figure 3.1. Schematic of the twisted tape inserts [59].

By first law of thermodynamics of the solar collector, the efficiency η_1 is obtained by [134].

$$\eta_I = \frac{Q_u}{\dot{Q}} = F_R\eta_0 - \frac{F_R U_L}{C_0}\left(\frac{T_{in}-T_a}{G_B}\right) \tag{3.7}$$

Since $\dot{Q}_.$ is the solar radiation reached the solar collector [59].

$$\dot{Q}_. = A_a G_B \tag{3.8}$$

Loss coefficient $U_L[\ \mathrm{W/m^2\ K}]$ presents the thermal losses from the receiver, which is depended on the area of the receiverA_r. The loss coefficient U_L for a plain tube receiver regarding the surface convection and radiation, and conduction through the structure can be neglected because it is isolated, is given by [59].

$$U_L = h_r + h_v \tag{3.9}$$

Where, h_v heat transfer coefficient and h_r linearized radiation coefficient, as a result of wind. The values of h_r can be calculated as [59].

$$h_r = 4\sigma\varepsilon_r T_r^3 \tag{3.10}$$

Where σ, ε_r, T_r are Stefan-Boltzmann constant, emissivity of the surface receptor and receiver surface temperature, respectively. If a single value of h_r is not adequate as a result of large temperature differentiation through the direction of flow, each with a constant h_r, wind loss coefficient h_v, [132].

The Zhukauskas relation is applied due to cross flow in the receiver is regarded [135].

$$\overline{Nu_D} = (B)(\overline{\mathrm{Re}_D})^m(\mathrm{Pr})^n\left(\frac{\mathrm{Pr}}{\mathrm{Pr}_r}\right)^{1/4} \tag{3.11}$$

Where the Reynolds number $1 < \mathrm{Re}_D < 10^6$, Re for a circular cylinder at crossflow,$\overline{\mathrm{Re}}_D$, obtained by [59].

$$\overline{\mathrm{Re}_D} = \frac{V_v D_0}{\nu} \tag{3.12}$$

Where V_v is the wind velocity and D_o is the receiver tube's outside diameter. The parameters in Eq. (3.11) can be estimated at the ambient temperature T_a. However the value of Pr_r depends on the receiver temperature T_r,where m and n is constant. If the P_r is $\mathrm{Pr} \leq 10$ then $n = 0.37$, and if. $\mathrm{Pr} > 10$, $n = 0.36$. Therefore, the estimation of h_v, is obtain by the relation [136].

$$h_v = \overline{Nu_D}\,\frac{k_v}{D_o} \tag{3.13}$$

Since k_v is the air thermal conductivity. To evaluate the coefficients h_r and h_v must be predicts the T_r. A first approaches to estimate T_r is over a balance of energy in the receiving tube regardless the heat losses to evaluate the value of T_r. The receiver tube is made of copper and has thin walls that are thought to have a high thermal diffusivity. Its inner and outside walls are meant to be at the same temperature, such as [59].

$$h_w(T_r - T_{\text{out}}) = \eta_o C_o G_B \tag{3.14}$$

T_{out} being the average temperature of the fluid at the outlet of the receiver tube. Therefore, is evaluated value of T_r is [59].

$$T_r = \frac{\eta_0 C_0 G_B}{h_W} + T_{\text{out}} \tag{3.15}$$

Since T_r, is considered to be constant. h_w, to the inside of the receiver obtained by following equation [137].

$$h_w = \frac{k_w Nu_D}{D_i} \tag{3.16}$$

Since the value of k_w could be given from [136], and D_i internal diameter of the receiver tube. To evaluate T_{out} in Eq. (3.15), the energy balance is considered [59].

$$\eta_o C_o G_B A_r = \dot{m} C_p (T_{\text{out}} - T_{\text{in}}) \tag{3.17}$$

Since T_{in}, inlet temperature at of the receiver tube. Finally, T_{out}, outlet temperature, receiver area, $A_r = piD_oL$ as follows [59].

$$T_{\text{out}} = \frac{\eta_0 C_0 G_B (\pi D_0 L)}{\dot{m} C_p} + T_{in} \tag{3.18}$$

The thermodynamic simulation model of solar collector is covered to treat with two cases for study:

- Empty tube.
- Twisted tape inserts in a tube.

When an empty tube is regarded, Eq.(3.16), given from the standard pipe flow equation [132].

$$Nu_{D_E} = 0.023(\text{Re})^{0.8}(\text{Pr})^{0.4} \tag{3.19}$$

Since the empirical correlation for the, Nu_{π} is known as the Dittus-Boelter equation for heating of the fluid, while, in the particular case of a swirl flow resulted from twisted tape inserts, h_w Eq. (3.16) could evaluated applying equation [59].

$$\text{N}u_{D_\pi} = 0.224(\text{Re})^{0.66}(\text{Pr})^{0.4}\left(\frac{y}{w}\right)^{-0.6} \tag{3.20}$$

Since $\text{N}u_{D_\pi}$ is the empirical correlation from [31] and the term y/w is twist ratio. Utilizing twisted tape insert at for specified $(2700 < \text{Re} < 21{,}000)$ this empirical correlation was provided. Test tube was fabricated of Cu The twisted tapes are inserted put at the tube's center along the tube to ensure a tight connection between the tapes and the tube without the need for extra fitting [31]. As a result of the twisted tape, advection and diffusion are both included in convection as a fin effect. The Prandtl number, Pr, for each study case defined by:

$$\text{Pr} = \frac{\nu}{\alpha} \tag{3.21}$$

Since (α) thermal diffusivity, (v) kinematic viscosity , Re is evaluated when empty tube [31].

$$Re = \frac{4\dot{m}}{\pi D_i \mu_w} \tag{3.22}$$

Since $(\dot{m})$, and, (μ_w)., F_R is evaluated in [132].

$$F_R = \frac{\dot{m}C_p}{A_r U_L}\left[1 - \exp\left(-\frac{U_L F' A_r}{\dot{m}C_p}\right)\right] \tag{3.23}$$

Since $(\dot{m})$, and (C_p), at constant pressure, the F' efficiency factor is obtained by [132].

$$F' = \frac{\frac{1}{D_L}}{\frac{1}{U_L} + \frac{D_0}{h_w D_i} + \left(\frac{D_0}{2k}\ln\left(\frac{D_0}{D_i}\right)\right)} \tag{3.24}$$

Since D_i and D_0 are the tube's internal and external diameters, respectively, and thermal conductivity (k) of the receiver tube. Clearly that Eq. (3.7) match to a standard linear equation pattern of $y = b + mx$, since $F_R\eta_0$ corresponds the y intercept and $F_R U$ corresponds the slope. It is worth noting that the linear fit instead than a second degree fit able in the solar collector for low temperature [132]. (ΔP) Pressure drop can be evaluated by [137]:

$$\Delta P = f\frac{4l}{D_i}\frac{\rho V_w^2}{2} \tag{3.25}$$

Where l length receiver tube, D_i initial diameter of the tube, f represents the friction factor, ρ fluid density, and $(V_w = \dot{m}/\rho A)$ fluid velocity. The friction factor correlation for the empty tube expresses as [31].

$$f_E = 0.376\ \mathrm{Re}^{-0.249} \tag{3.26}$$

Whereas, the twisted tape's friction factor is evaluated by [31].

$$f_{TT} = 65.4\mathrm{Re}^{-0.52}\left(\frac{y}{w}\right)^{-1.31} \quad (3.27)$$

3.3. NUMERICAL MODEL

The following is how the incompressible flow liquids continuity equation is described. [136].

$$\frac{\partial}{\partial x}(\rho u_i) = 0 \quad (3.28)$$

Concerning the heat conduction, the different materials, and the energy equation can be obtained by [138].

$$K_m\left(\frac{\partial^2 T}{\partial x^2} + \frac{\partial^2 T}{\partial y^2} + \frac{\partial^2 T}{\partial z^2}\right) = 0 \quad (3.29)$$

Whereas, the equation of energy can be expressed as [139].

$$\nabla(\rho h\vec{U}) = -p\nabla\vec{U} + \nabla(k\nabla T) + \phi + s_h \quad (3.30)$$

Finally, Navier-Stokes equations of the three dimensional can be as illustrate at Eq. (3.53) [139].

$$\begin{aligned}
\nabla\cdot(\rho\vec{U}u) &= -\frac{\partial p}{\partial x} + \frac{\partial \tau_{xx}}{\partial x} + \frac{\partial \tau_{yx}}{\partial y} + \frac{\partial \tau_{zx}}{\partial z} \\
\nabla\cdot(\rho\vec{U}v) &= -\frac{\partial p}{\partial y} + \frac{\partial \tau_{xy}}{\partial x} + \frac{\partial \tau_{yy}}{\partial y} + \frac{\partial \tau_{zy}}{\partial z} \\
\nabla\cdot(\rho\vec{U}w) &= -\frac{\partial p}{\partial z} + \frac{\partial \tau_{xz}}{\partial x} + \frac{\partial \tau_{yz}}{\partial y} + \frac{\partial \tau_{zz}}{\partial z}
\end{aligned} \quad (3.31)$$

The efficiency (PTC) can evaluate from the useful heat Q_u and the solar energy Q_s that fell on a collector aperture area in an equation:

$$Q_u = F_r(\eta_o A_a G_B - A_r U_L(T_s - T_a) \quad (3.31)$$

$$Q_s = A_a G_B \quad (3.32$$

Thermal efficiency equation Eq. (3.33):

$$\eta_I = Q_u/Q_s \tag{3.33}$$

PART 4

METHODOLOGY

4.1. PHYSICAL MODE AND BOUNDARY CONDITIONS

In this study, heat transfer fluid (HTF) is water, and it enters the tube in a laminar flow with a Re <2300. It was constructed of aluminium, the twisted tape., the twisted tape's characteristic geometries, measured in length (L) and thickness (t). As Figure 4.1. Illustrates twist ratio (y/w). (y) corresponding twisted tape pitch and (w) corresponding height of tape ratio. To investigate the impact of twisted tape, three value of it is applied as shown in Figure 4.1. The hydraulic and thermal parameters of the working fluid, pure water, are shown in Table 4.3. Water enters the tube at 293 K. Fluid flow is laminar and the range of Re 500,1000 and 1500. Uniform velocity and fully develop is assumed in the simulation model, length of the tube in Table 4.1. Copper was used to make the absorber tube because it has a higher thermal conductivity (k=380.5W/m.K). As compared to steel and aluminium. In order to maximize thermal efficiency, absorptivity (0.96), and reduce radiation heat transfer loss from the absorber tube with transmissivity, the outer surface of the absorber was coated in black. This caused it to function similarly to a black body ($\varepsilon \approx 1$), which absorbs heat more efficiently than other colored bodies (0.80). While the twisted tape, walls are contact with air, that moves with velocity at 2.3 m/s and temperature (293 K). A heat flux of 865 w/m^2 is expose uniformly to the tube surface. The tube outlet also uses a pressure outlet condition, as well as properties for cooper-based alloy.

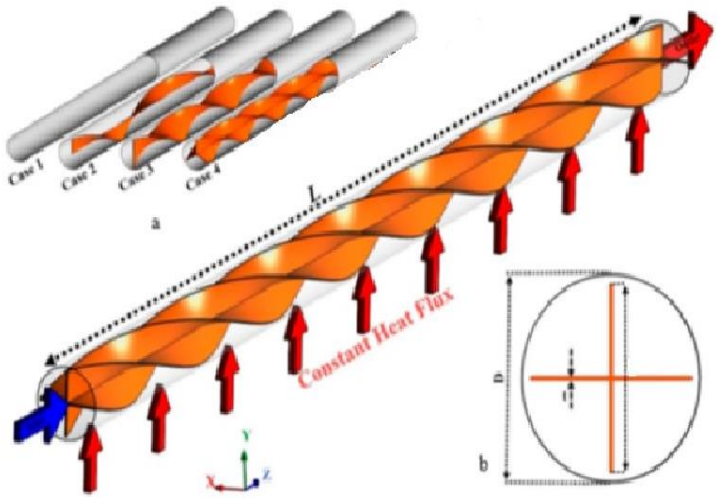

(a)

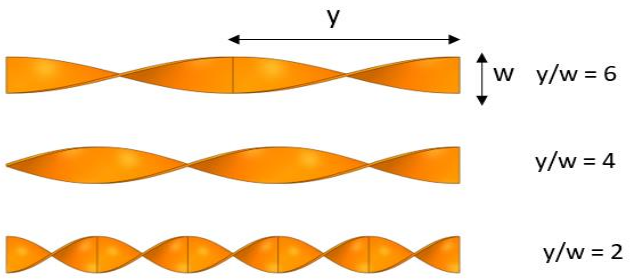

(b)

Figure 4.1. (a) Diagram of the proposed system for boundary condition [83].(b) The dimension of the studıed system. different twisted tape pitches.

Parabolic Trough Collector **(**PTC) was made with reflectivity (0.92), the parabolic mirror's total area, with length (L), width (W), the distance between the reflector and absorber tube is known as the focal length (f), the angle formed by a focal point's line and a parabolic service edge's vertical axis is known as the rim angle (ϕ), As illustrate Figure 4.2. Table 4.1 shows its main parameters. The aim of this standard is to define test procedures for calculating thermal performance of single-phase fluid solar energy collectors. This technique is frequently used to calculate thermal efficiency and compare it to thermal efficiencies of similar solar collectors.

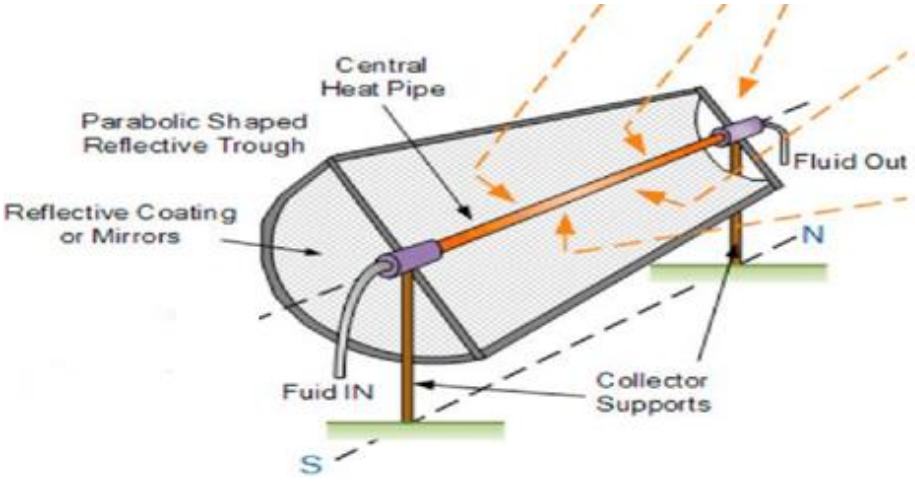

Figure 4.2. Dimensions of a parabolic trough collector PTC [140].

Table 4.1 Geometrical parameters' dimensions.

Parameter	Values
Aperture area,A_a	5.187 m^2
Receiver area,A_r	0.389 m^2
External diameter for the absorber tube,D_o	2.54 cm
Internal diameter for the absorber tube, D_i	2.32 cm
Length of the parabolic reflector, L	4.88 m
Aperture width, W_a	1.063 m
Tape width, w	0.023 mm
Twist ratio, y/w	2,4,6
Concentration ratio, C_o	13.3
Focal length, f	0.26 m
Rim angle, ϕ	90^0
Absorptivity for an absorber tube, α_r	0.96
Emissivity, ε	0.96
Reflectivity for a parabolic mirror, ρ	0.92
Optical efficiency, η_o	0.70

4.2. CODE AND CONVERGENCE

The commercial ANSYS FLUENT computational fluid dynamics (CFD) code (version 2020 R2) software to conduct a parametric study on the geometry of Parabolic trough concentrator (PTC). In order to analyse the efficiency improvement brought about by twisted tape inserts. The geometry and grid for this study are generated using design Ansys meshing. Along with recording mass-weighted magnitudes of average velocity and temperature for the tube output, the convergence conditions for energy equations are also taken into account. Solution method the governing equations' solutions and the corresponding boundary conditions were obtained utilizing both optical investigations carried out using CFD tools. Previous studies have been discussed the methodological aspects of the optical analysis utilized to produce the actual heat flux profile shown in Figure 4.1. The workbench workflow in ANSYS FLUENT was used to implement the solution. In ANSYS design, the geometry shown in Figure 4.2 was modelled. Utilizing the ANSYS meshing tool, the computational domain was modelled and discretized. Tetrahedral mesh for boundary layer resolution using prism layers was chosen due to the computational domain's complexity. In Figure 4.3, high mesh densities around the insert and the prism layers on both the inside wall of the absorber tube and the insert are visible in the study's mesh improvement of water flow distribution, water velocity and temperature inside a tube containing a twisted tape was numerically investigated using 3D CFD ANSYS FLUENT code.

4.3. MESH STUDY AND ANALYSIS

The domain was meshed using ANSYS software. Figure 4.3 shows the cross-section of the structural mesh generated for this investigation on a long pipe with twisted tape. Table 4.2. Contains many mesh sensitivity tests, to verify that the results are grid-independent. For grid independency analysis in the situation of fully filled twisted tape, several cell numbers are investigated., the number of unstructured cells (tetrahedrons and hexahedrons) was taken between (45,828) and (4,756,024) cell. The selection criterion shown in Table 4.2. is the average Nu, since applying finer meshing results in relative errors of less than one percent for outlet temperature and when the number

of elements exceeds these amounts, no effect on the results can be achieved, case (8) at (1809950) cell number is chosen for all simulations as indicated. With ANSYS meshing, a completely organized mesh is produced as demonstrated, resulting in high quality, quick convergence, and reduced computational time in the CFD FLUENT code.

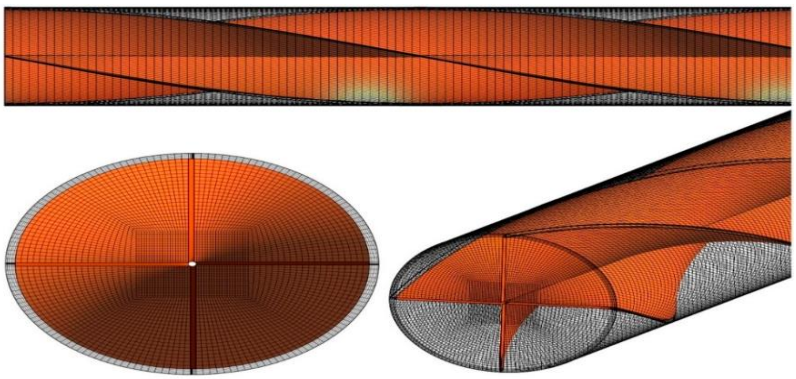

Figure 4.3. The computational domain's meshing.

Table 4.2. Analysis of mesh independence.

Case	Cell Number of Elements	Nu	(%)
1	45828	4.79931	----
2	164780	4.78936	0.207752
3	289006	4.7486	0.858358
4	454034	4.71999	0.606145
5	636504	4.68227	0.805592
6	1015341	4.66196	0.435654
7	1274499	4.635	0.581661
8	1809950	4.61931	0.339661
9	3129110	4.61914	0.00368
10	4756024	4.616	0.068024

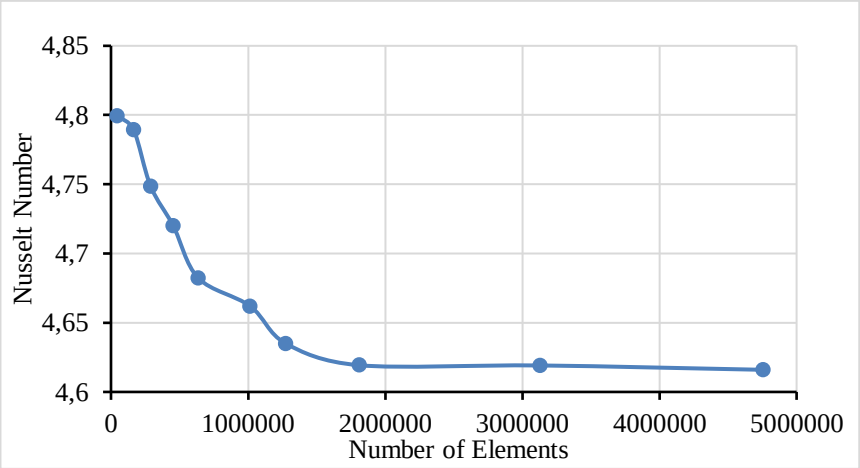

Figure 4.4. Mesh analysis.

4.4. NUMERICAL MODELING AND ANALYSIS

CFD numerical modelling process was proposed in this thesis. This section is demonstrated the dominant equations with actual conditions, where the receiver tube have laminar flow. This is assists in decreasing receiver tube temperature gradients to save the observer tube from thermal stresses and definitive failure, as well as ensures better heat transfer coefficients in turn enhanced performance.

We utilize ANSYS Fluent (CFD) to execute simulations and solve equations once the geometrical model is confirmed. For the numerical validation we consider three different twist ratios y/w (2,4, and 6), each of which operates at a different mass flow rate. While simulation the pressure drop and heat transfer rate are determined under fully developed circumstances for different (Re) (1500,1000 and 500) laminar fluid flow based on the mean flow velocity and the tube diameter. Since the Nu specifies the proportion to conductive heat transfer through the tube, we start by examining its behaviour. For PTC systems, the thermal efficiency was determined. Show how efficiently insert materials to improve thermal performance is shown by the thermal efficiency of the system. For the theoretical model to be implemented, we consider two study cases:

4.4.1. Numerical Modelling Nusselt Numbers for Thermally Developing Laminar Flow of the Empty Tube

To validate the presented findings, it is note that the copper PTC tube and copper strip used to make the twisted tapes were both used. In Table 4.3 provides the main key of the theoretical model's important elements as they relate to the thermophysical characteristics of saturated water at (1.21atm), and air 20 C at 1atm pressure methods for thermally producing laminar flow in circular ducts are studied. It is shown that the Nusselt number depending on the square root of the cross sectional flow rate area is a weak function of the shape of the geometry provided an appropriate aspect ratio is defined. It is also shown that there are two distinct bounds for the fully developed Nu which depend upon shape and symmetry of the geometry. A general model which is valid for many duct configurations is developed by combining for the thermal entrance region where the flow asymptote has fully developed. The model is simpler than other general models and provides equal or better accuracy. A obvious choices for a characteristic length are the perimeter the square root of the flow area $L = \sqrt{A}$. Finally, it is shown that the solution for the circular duct geometry may be used to accurately results for Nusselt Number with an accuracy of ±12 percent as in Figure 4.5 [141].

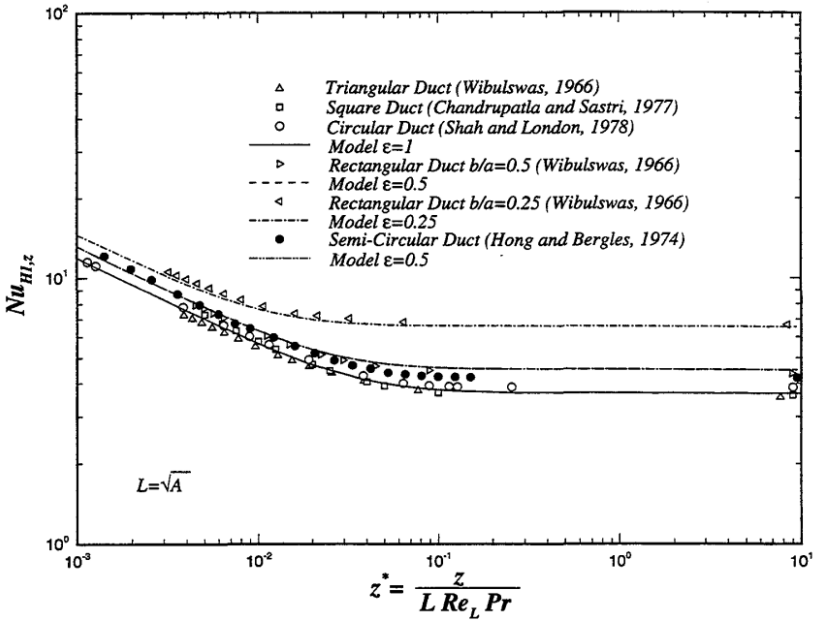

Figure 4.5. Thermally developing for the laminar flow of the empty tube Nu [141].

4.4.2. Numerical Equations for The Lamınar Flow of an Empty Tube with A Twisted Tape Insert

For the Re ranging (500,100,1500), the alternating clockwise and counter clockwise twisted-tape circular tubes' thermohydraulic characteristics are described. In the model, the twisted tapes were individually put into the uniform wall heat flux with three distinct twist ratios y/w (2, 4, and 6). The working fluid was water. Given that all of the thermal performance factors calculated using the same pumping power are greater than unity, Heat transfer enhancement has been found to be effective. Additionally, the empirical correlations for the thermal performance factor, friction factor, and Nu have been developed. Model ANSYS Fluent for Nu and for thermal performance factor (η) is shown to be in good agreement with the resultant from the correlations. In order to evaluate the heat transfer enhancement and the pressure drop increase produced by the twisted tapes, comparisons of the reference data of heat transfer and friction factor in the smooth circular tube with fully developed thermal flow were obtained. With increasing Re, (Nu) significantly rises, indicating an increase in convective heat transmission. This trend runs counter to what is typical in a turbulent regime. This directly associated to the variation in thermal boundary layer thicknesses between these two regimes. In the laminar regime. The thermal boundary layer is thick, thus shear accords also increases with flow velocity increases, amplifying the disturbance of the boundary layer. Depending (Nu) for the tube insert twisted tape on twist ratio (y/w) and (Re). The implications of the model on the laminar flow regime behaviours of uniform wall heat flux tubes' heat transfer, friction factor, (Nu), and thermal performance are explained. To assist in the design and retrofit applications of the use tube with a twisted tape inserts for the laminar region, the numerical findings were submitted to the empirical correlation development. The main conclusions can be in Eq. (4.1) [142].

$$Nu = 0.005 Re^{1.139} Pr^{0.4} (Y/w)^{-0.521} \quad (4.1)$$

Table 4.3. Use of Relevant values during the modeling process.

Fluid Properties	Quantity
Density, ρ_w	992.23 kg/m^3
Dynamic viscosity, μ_w	0.653 x 10^{-3} kg/m.s
Heat capacity, C_{pw}	4.1785 kJ/kg.K
Kinematic viscosity, v_w	0.659 x 10^{-6} m^2/s
Kinematic viscosity, v_{air}	0.153 x 10^{-6} m^2/s
Thermal conductivity, k_{air}	0.0263 W/m.K
Thermal conductivity, k_w	0.631 W/m.K

PART 5

RESULTS AND DISCUSSION

5.1. MODEL VALIDATION PROCEDURE

Figure 5.1 shows the comparison between the current numerical results and the model ANSYS FLUENT data available for Nusselt number for empty tube containing fluid flow and heat transfer in a pipe filled with a pure water for different Reynolds numbers Re (500,1000 and 1500) laminar fluid flow according to the tube's diameter and mean flow velocity. Overall considering the Figure 5.1, it is concluding that the numerical procedure was acceptably performed. The disparity is about 24.8% for Re (500), 9.8% for Re (1000) and 6.9% for Re (1500), Nusselt number and Reynolds numbers are shown in Figure 5.1.

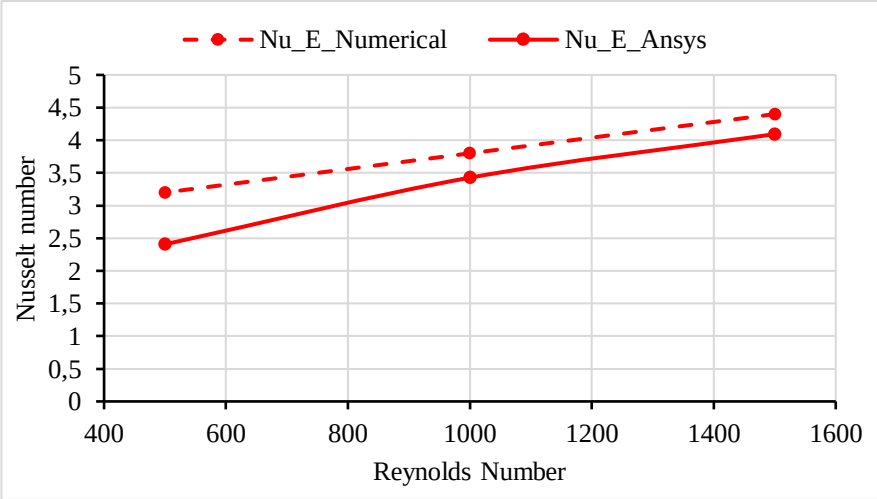

Figure 5.2. Comparison between the Ansys fluent data and current numerical results for the Nu.

Figure 5.2 shows the comparison between the current numerical results and the model ANSYS FLUENT data available for Nu for tube containing fluid flow and heat transfer in a pipe filled with a pure water and containing a twisted tape(y/w=2) for different Re (500,1000 and 1500) laminar fluid flow according to the tube's diameter and mean flow velocity. Overall considering the figure, it concludes that the numerical procedure was acceptably performed. The disparity is about 17.5% for Re (500), Re (1000) and Re (1500), Nusselt number and Reynolds numbers are shown in Figure 5.2.

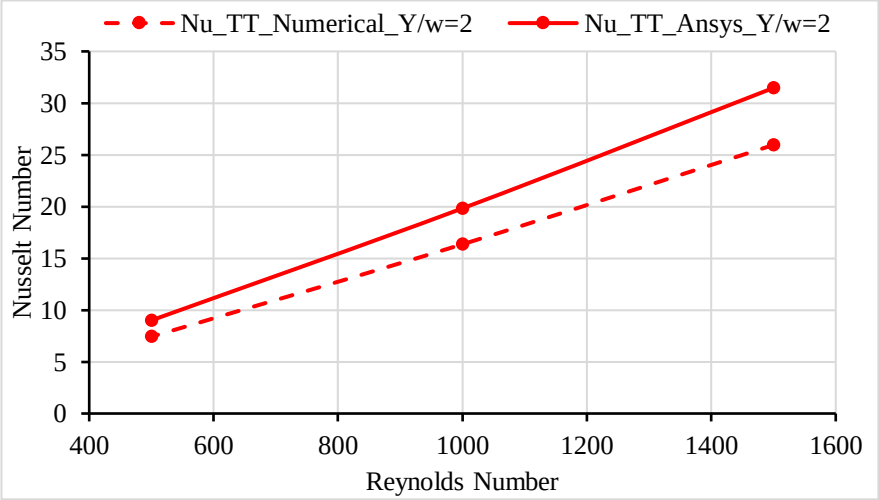

Figure 5.3. Comparison between the Ansys fluent data of and current numerical results for the Nu.

Figure 5.3 shows the comparison between the current numerical results and the model ANSYS FLUENT data available for Nu for empty tube containing fluid flow and heat transfer in a pipe filled with a pure water and containing a twisted tape (y/w=4) for different Re (500,1000 and 1500) laminar fluid flow according to the tube's diameter and mean flow velocity. Overall considering the Figure 5.3, it concludes that the numerical procedure was acceptably performed. The disparity is about 17.5% for Re (500), Re (1000) and Re (1500), Nusselt number and Reynolds numbers are shown in Figure 5.3.

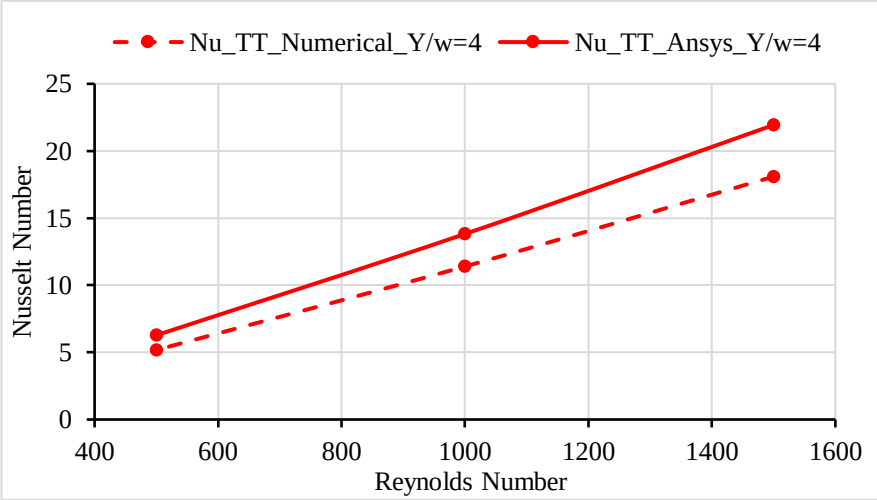

Figure 5.4. Comparison between the Ansys fluent data of and current numerical results for the Nu.

Figure 5.4 shows the comparison between the current numerical results and the model ANSYS FLUENT data available for Nu for empty tube containing fluid flow and heat transfer in a pipe filled with a pure water and containing a twisted tape (y/w=6) for different Re (500,1000 and 1500) laminar fluid flow according to the tube's diameter and mean flow velocity. Overall considering the figure, it concludes that the numerical procedure was acceptably performed. The disparity is about 17.5% for Re (500), Re (1000) and Re (1500), Nusselt number and Reynolds numbers are shown in Figure 5.4.

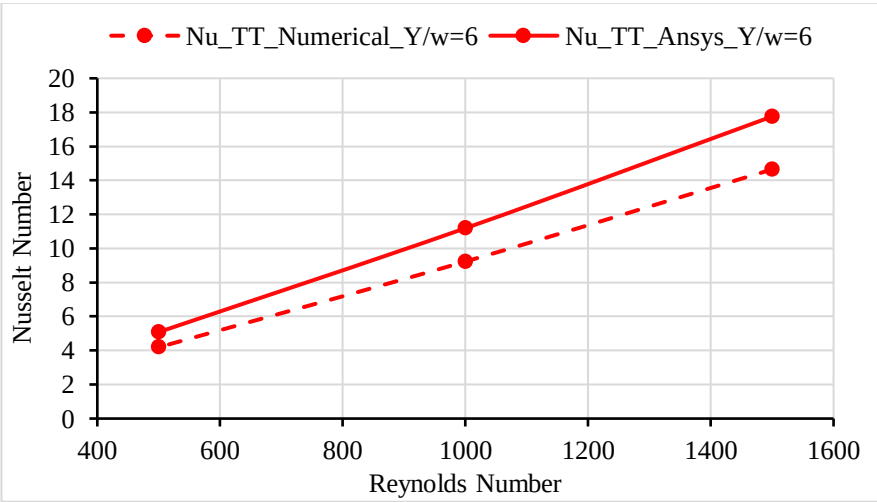

Figure 5.5. Comparison between the Ansys fluent data of and current numerical results for the Nu.

5.2. COMPUTATIONAL BASED NUMERICAL RESULTS

Figure (5.5), (5.6), (5.7) show the cross-sectional radial velocity contours for the cases of empty tube and twisted tape inserts y/w (2,4, and 6) in a cross-section for Reynolds number Re (500,1000, and 1500). The streamlines coloured by velocity magnitude are illustrated for value the three-twisted tape inserts y/w (2,4, and 6). It is visible that the flow path changes as the value of the twisted tape varies. While utilizing twisted tape, the radial velocity increases for cross-sectional values, causing the stronger secondary flows seen in Figure (5.5), (5.6), (5.7) in instances of twisted tape. Because more swirl flow fronts can be seen in twisted tape y/w=2 values with higher radial velocity, And the velocity decreases at the twisted tape y/w (2,4), Stronger secondary and mixing flow, hence. As a result, the core's colder fluid is more actively directed towards the hot wall, increasing the amount of heat transfer between the wall and the fluid.

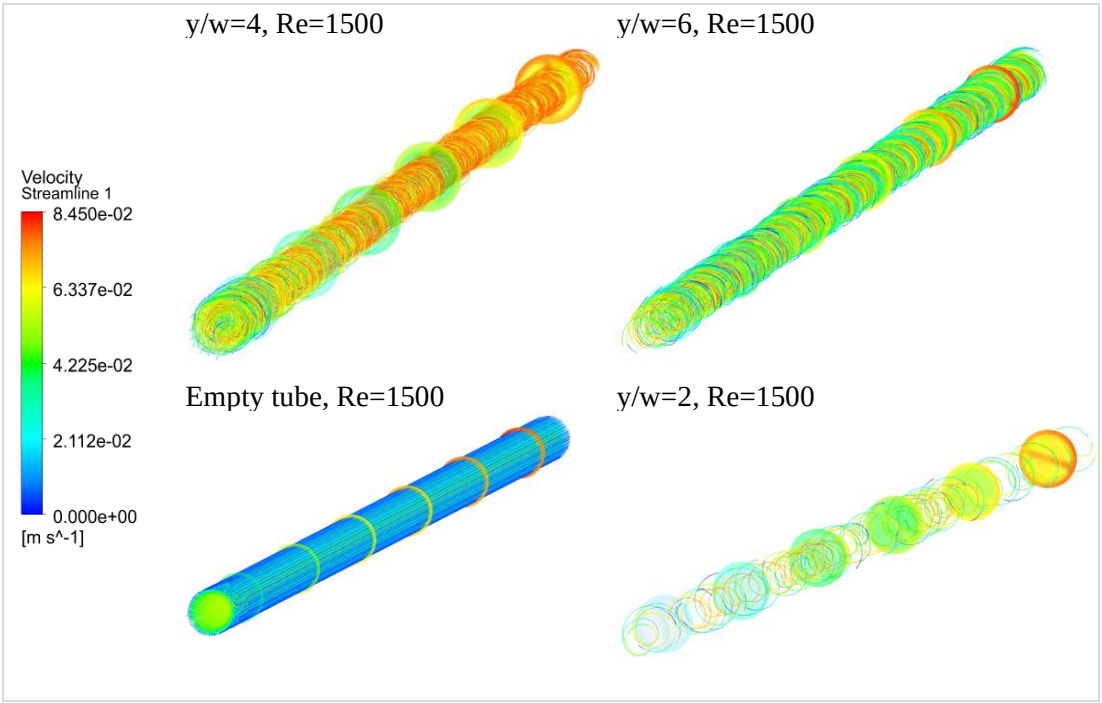

Figure 5.6. Streamline coloured by velocity magnitude for empty tube and twisted ratio y/w (2,4, and 6) for at Re=1500.

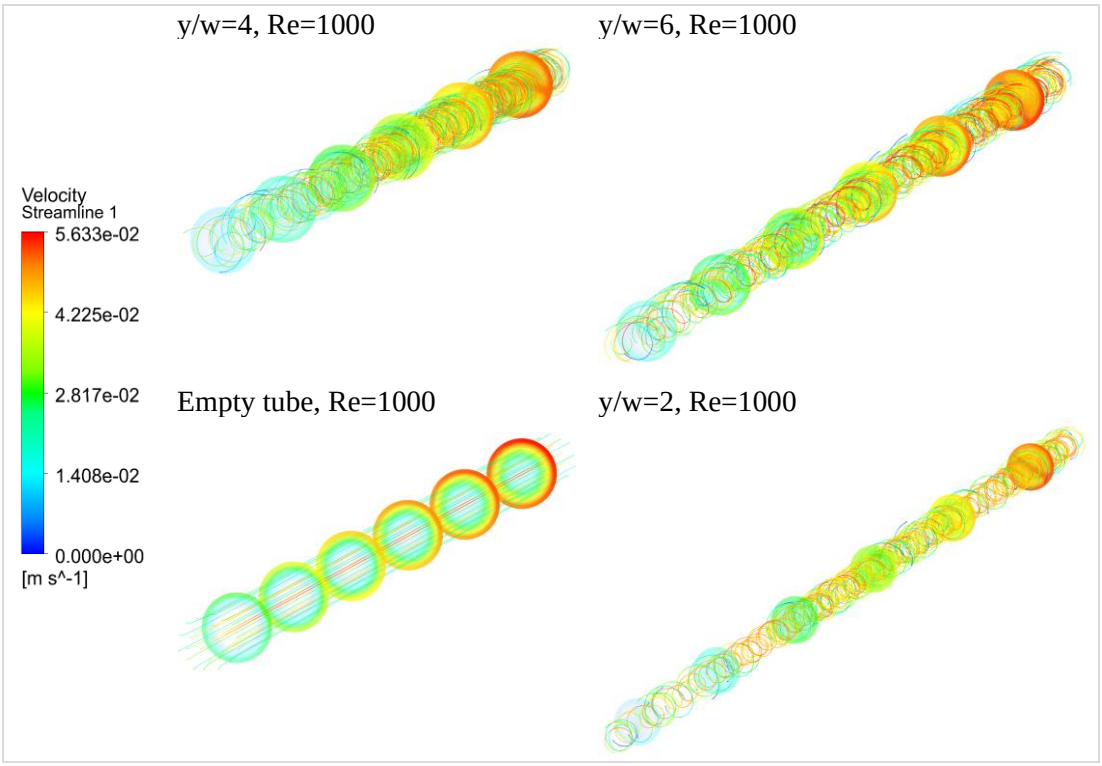

Figure 5.7. Streamline coloured by velocity magnitude for empty tube and twisted ratio y/w (2,4, and 6) for at Re=1000.

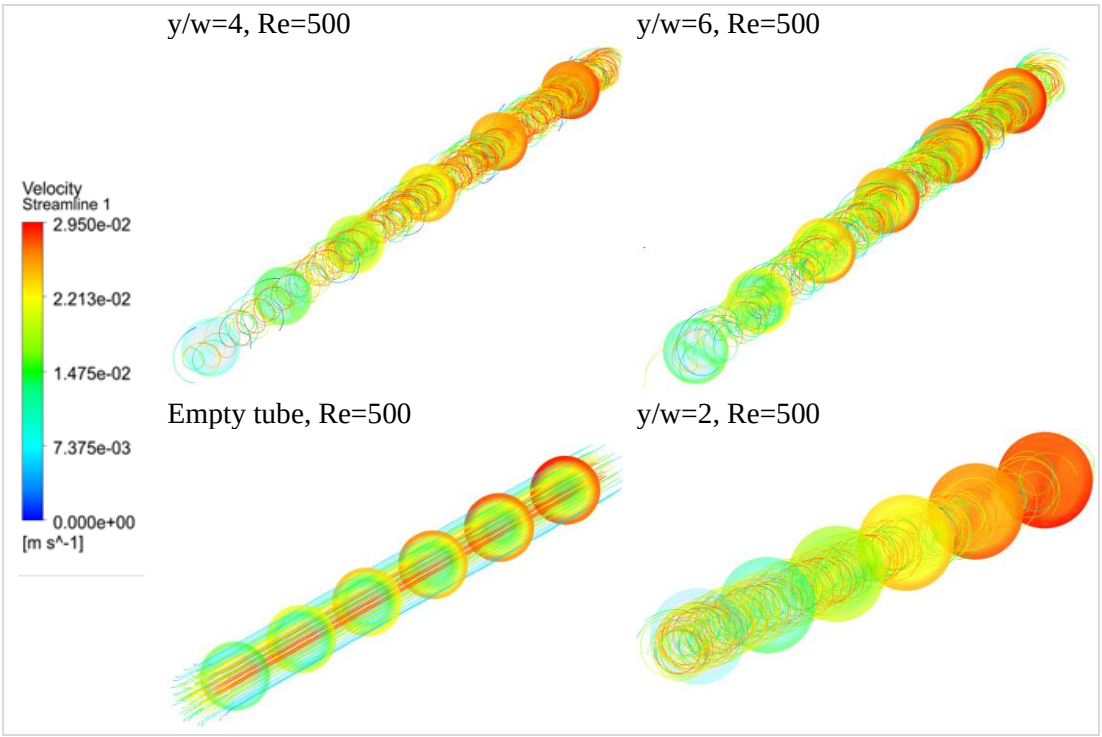

Figure 5.8. Streamline coloured by velocity magnitude for empty tube and twisted ratio y/w (2,4, and 6) for at Re=500.

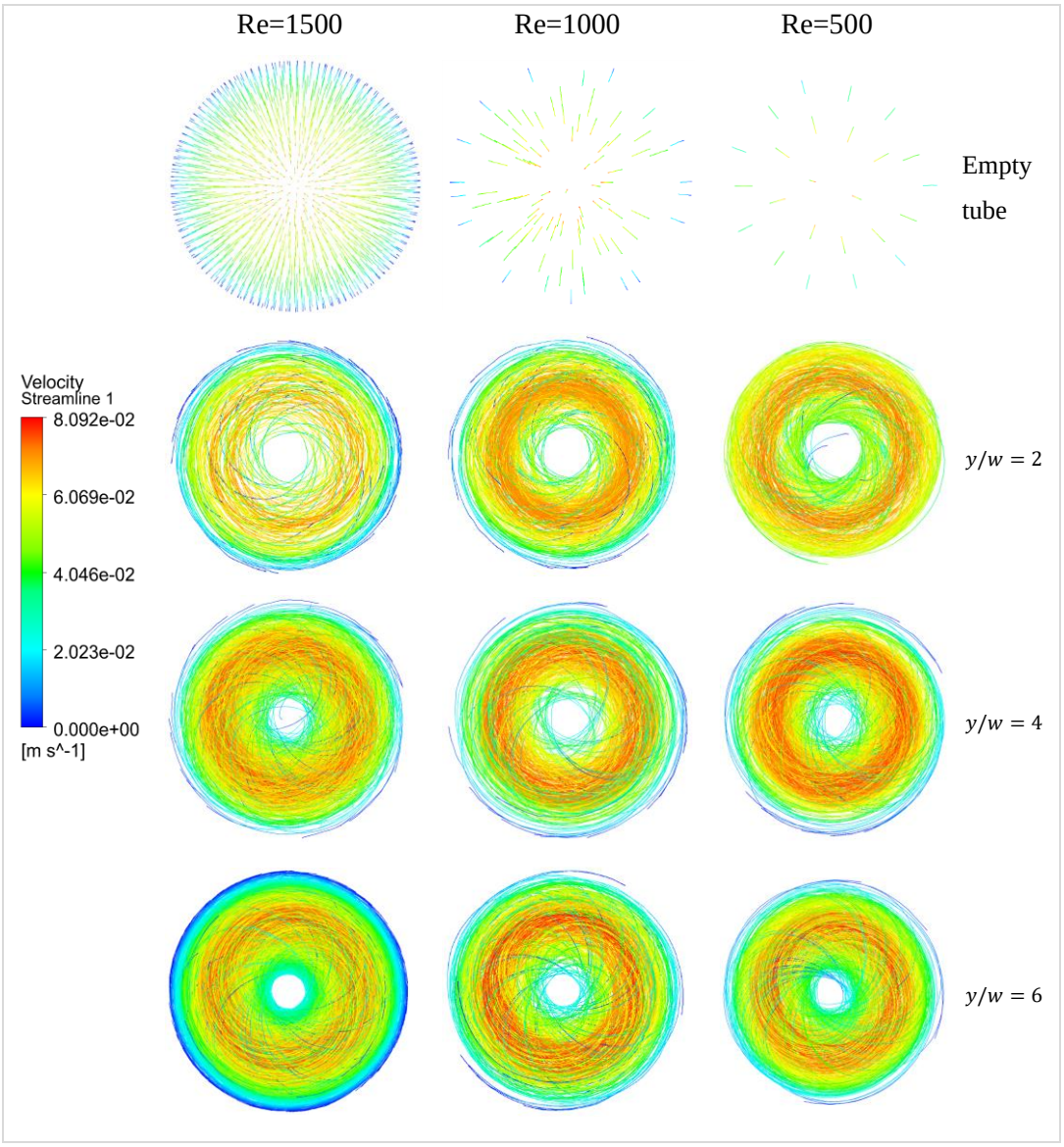

Figure 5.9. Cross-sectional velocity contours for empty tube and twisted ratio at y/w=2,4, and 6 at Re=500,1000,1500.

Figure 5.9 shows the average velocity curve for each twisted tape was illustrating the values of tangential velocity in terms of cases empty tube and twisted tape inserts y/w (2,4, and 6) in a cross-section for Reynolds number Re (500,1000, and 1500). From the results, it shows that the optimum twisted tape y/w=2 at a higher average velocity for the Reynolds number (Re) is 1500 with 0.005 m/s, compared to others. As can be seen, when y/w (4,6) is used, the radial velocity values in the tube cross-section are rather low. It is clear that using twisted tape and increasing its angular velocity has a considerable impact on the flow pattern at all of the selected points.

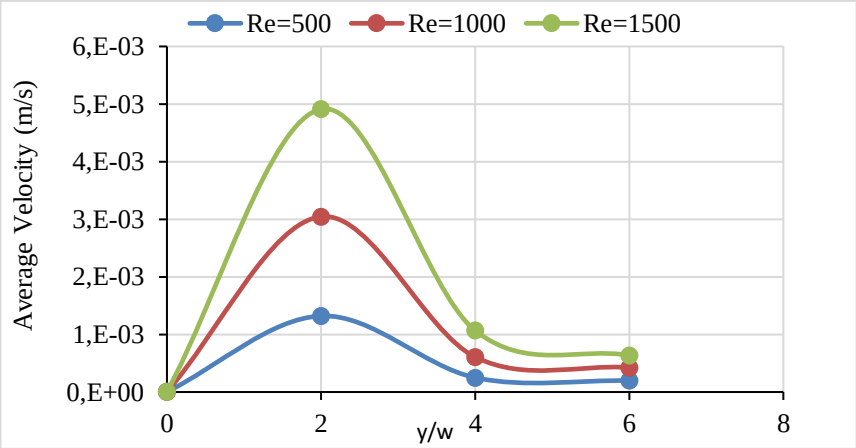

Figure 5.10. Average velocity profile for different four cases empty tube and tube insert twisted tape y/w (2,4, and 6) at for Re (500,1000, and 1500).

Figure 5.10 shows that surface temperature was made different effect contours for the cases of empty tube and twisted tape inserts y/w (2,4, and 6) in a cross-section for Reynolds number Re (500,1000, and 1500). The wall temperature was made different effect in Figure 5.11, where inserting a twisted tape into a water tube was recorded greater surface temperature for empty tube without twisted tape. Found wall surface temperature low at after insert twisted tape to the water tube. Figure 5.10 illustrate the temperature of the case of the empty tube was found higher than the three cases of the twisted tape. From the results, it shows that the optimum case empty tube at a higher wall temperature for the Reynolds number (Re) is 1500 at 328 K, compared to others. As can be seen, when y/w (2,4, and 6) is used, the values of the wall temperature are rather low in the tube, and the lowest surface temperature of the twisted tape y/w=2 for the (Re) is 1500 at 310 K. This indicates an increase in heat absorption through the tube surface to the fluid in the case of the twisted tape, especially for the twisted tape.

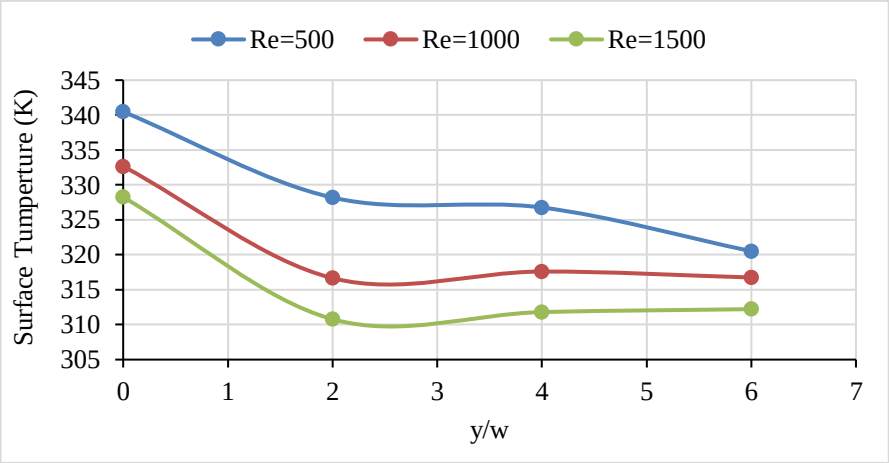

Figure 5.12. Changes surface temperature for different four cases empty tube and tube insert twisted tape y/w (2,4, and 6) at for Re (500,1000, and 1500).

Figure 5.11 shows the friction factor curve for each twisted tape was illustrating the values of friction factor in terms of cases empty tube and tube insert twisted tape y/w (2,4, and 6) for Re (500,1000, and 1500), of the results, it shows that the friction factor value is low in the case of the empty tube for Re (500,1000, and 1500) with friction factor (0.05,0.03 and 0.02) successively, and increases in the case of the insert twisted tape y/w (2,4, and 6), respectively, in the case of the Re (500,1000, and 1500). As can be seen, twisted tape y/w=2 at a higher friction factor for the Re is (500,1000, and 1500) with friction factor (0.28, 0.18, and 0.13) compared to others.

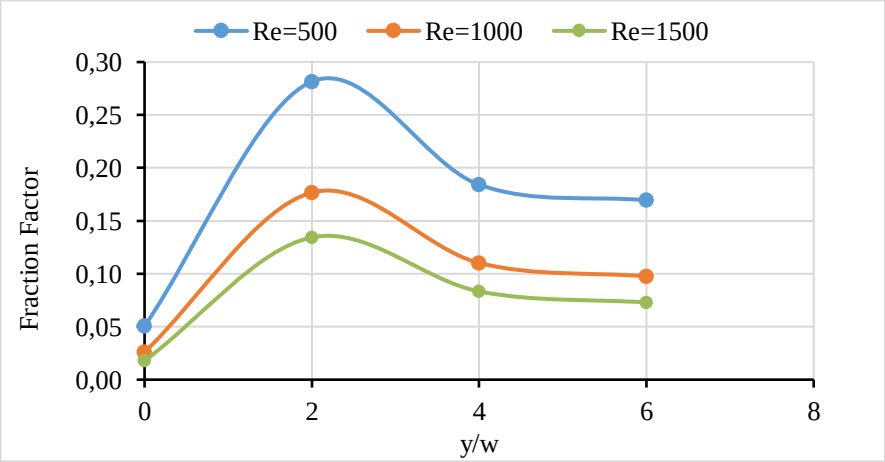

Figure 5.13. Changes friction factor for different four cases empty tube and tube insert twisted tape y/w (2,4, and 6) at for Re (500,1000, and 1500).

Figure 5.12 shows the cross-sectional pressure contours for the cases of empty tube and tube insert twisted tape y/w (2,4, and 6) in a cross-section for Reynolds number Re=1500. In which colored by the pressure magnitude are illustrated for value the three twisted tape y/w (2,4, and 6). It is visible that as the twisted tape value different, the flow path undergoes more changes. While utilizing twisted tape, the radial velocity increases for cross-sectional values, causing the stronger secondary flows seen in Figure 5.12. in instances of twisted tape. This is because more swirl flow fronts can be seen in twisted tape y/w=2 values with higher the pressure, and the pressure decreases at the twisted tape y/w (2,4).

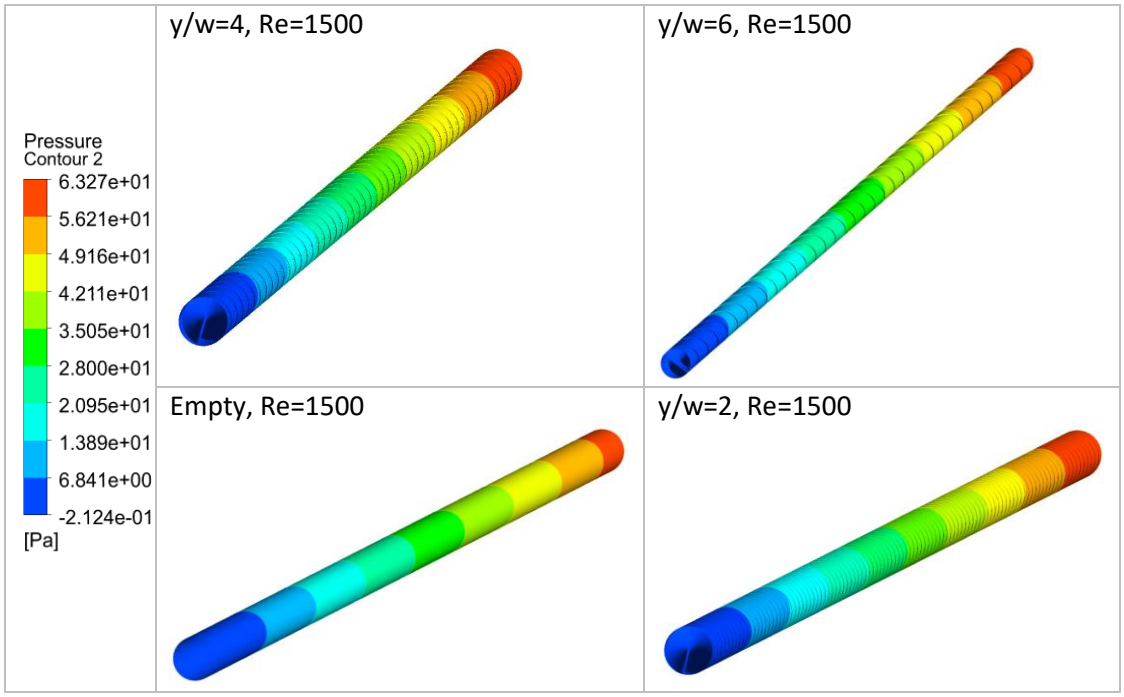

(a)

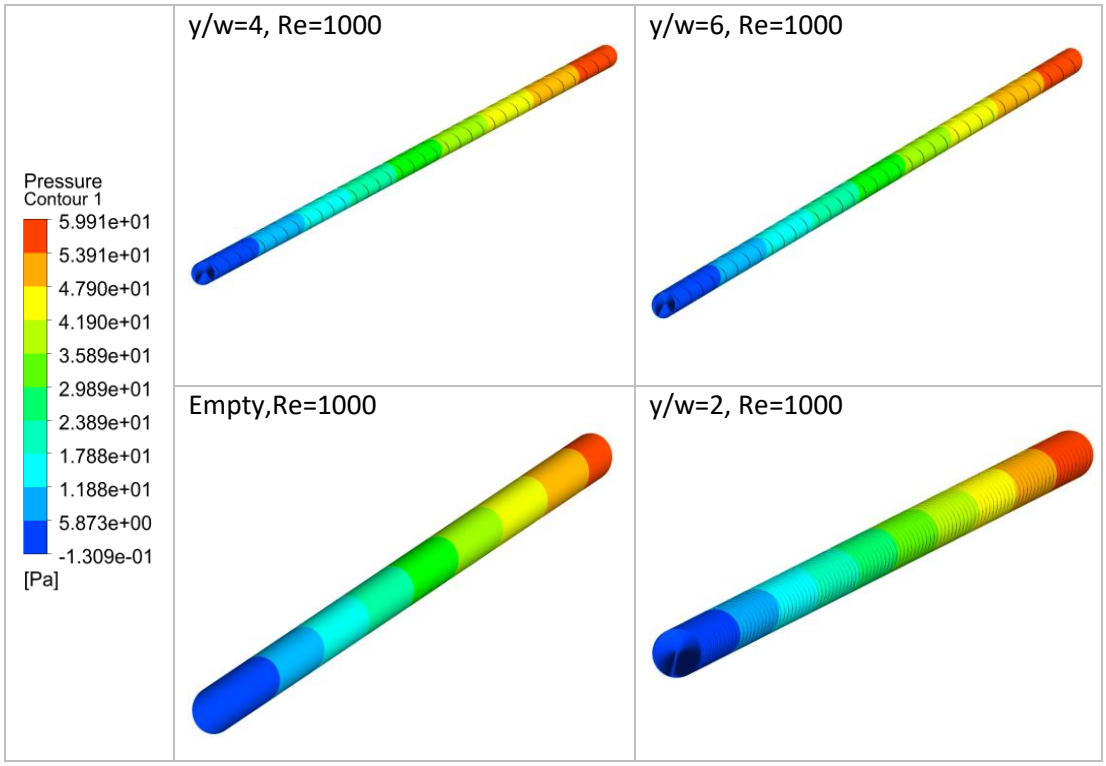

(b)

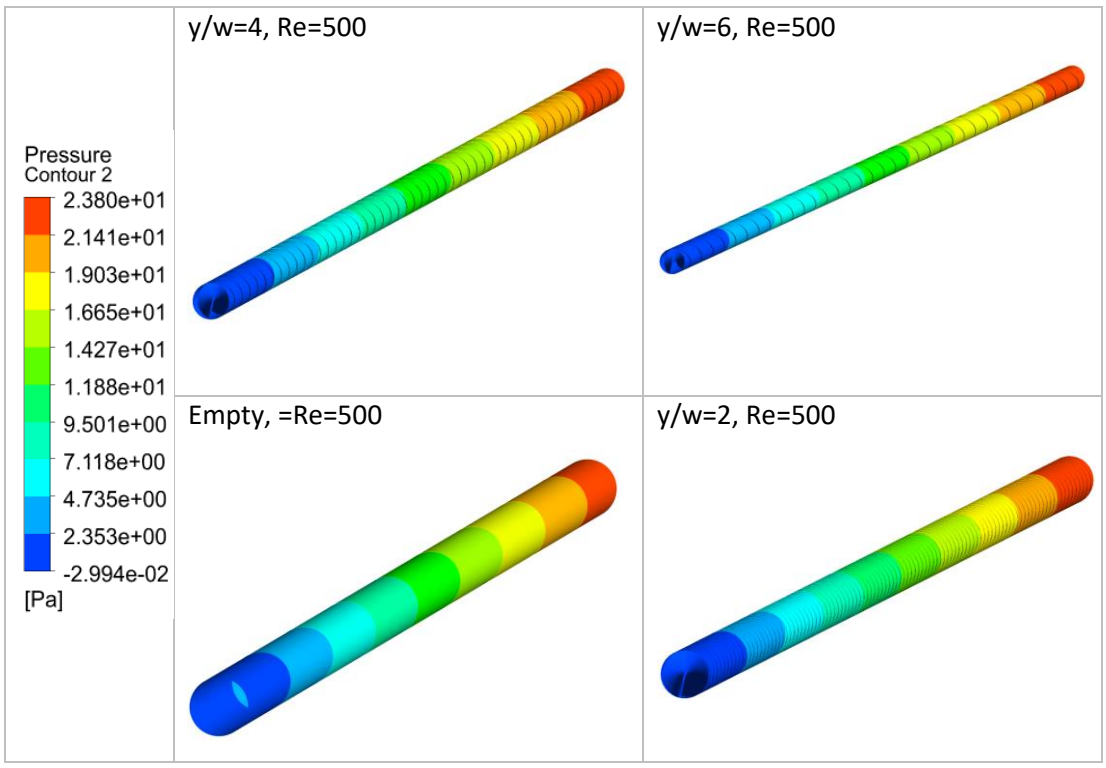

(c)

Figure 5.14. Pressure for different four cases empty tube and twisted tape inserts y/w (2,4, and 6) at Re 1500 (a),1000 (b), and 500 (c).

Figure 5.13 shows the average pressure curve for each twisted tape was illustrating the values of average drop pressure in terms of cases empty tube and tube insert twisted tape y/w (2,4, and 6) for Re (500,1000, and 1500). From the results, it shows that the average pressure value is low in the case of the empty tube for the Re is (1500, 1000, and 500) with average pressure (13.5, 8.8, and 4.3) Pa successively, and increases in the case of the insert twisted tape y/w (6,4, and 2), respectively, in the case of Re (500,1000, and 1500). As can be seen, twisted tape y/w=2 at a higher average drop pressure for the Re is (500, 1000, and 1500) with average pressure (101.8, 59.5, and 23.7) Pa successively compared to others.

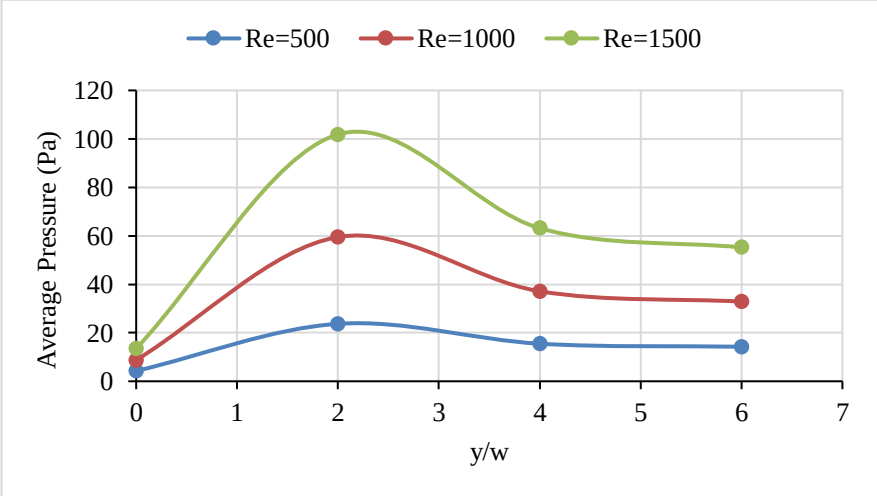

Figure 5.15. Changes average pressure for different four cases empty tube and twisted tape inserts y/w (2,4, and 6) at Re (500,1000, and 1500).

Figure 5.14 shows the cross-sectional temperature contours, at different wall for empty tube and twisted tape inserts at Re of (500,1000, and 1500). The thermal boundary layer develops normally over the length of the tube as seen by the empty tube cross sectional temperature contours. Because there is no method to improve heat transfer, such as a passive or active manner, the water temperature does not effectively well in the centre of the tube with the heat coming from the collector. After inserting the twisted tape, the centre of the tube gradually warms up as a result of the twisted tape because the severe turbulence caused the water at the surface to swirl and mix with the centre tube. As can be seen, twisted tape y/w=2 at a higher temperature distribution for the Reynolds Number (Re) is (500, 1000, and 1500) with outlet temperature (343K) successively compared to others.

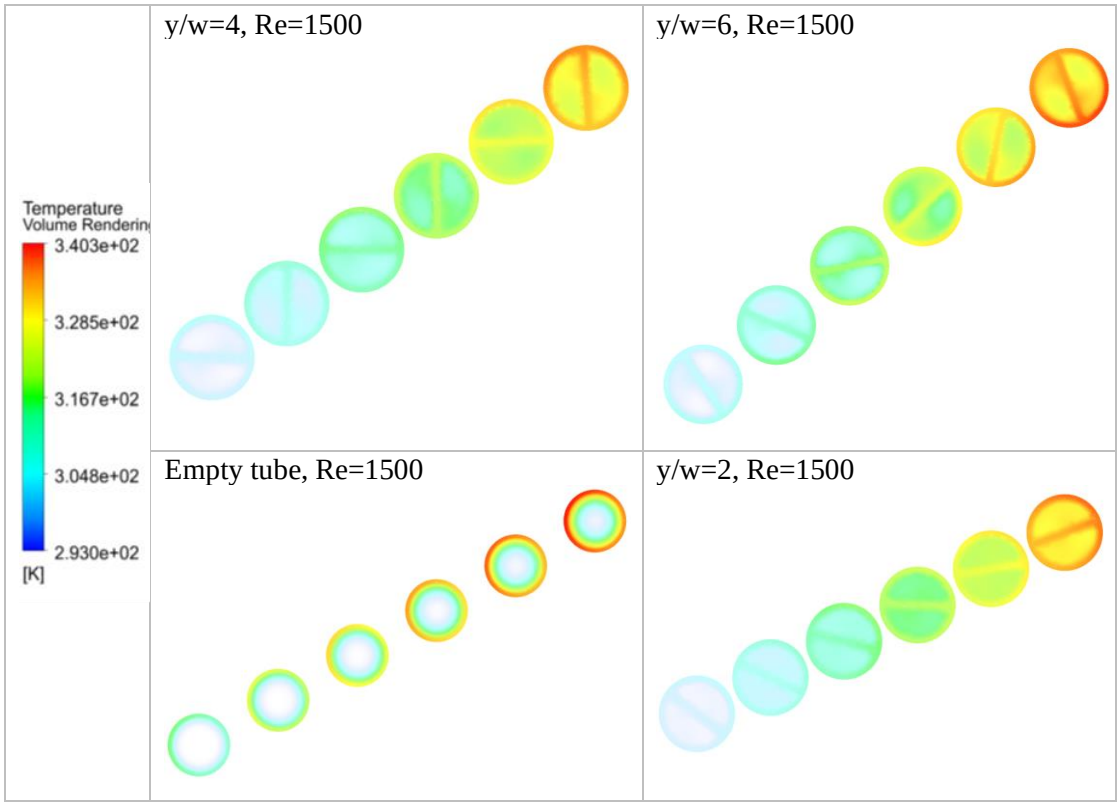
Temperature
Volume Renderin
3.403e+02
3.285e+02
3.167e+02
3.048e+02
2.930e+02
[K]
y/w=4, Re=1500
y/w=6, Re=1500
Empty tube, Re=1500
y/w=2, Re=1500

(a)

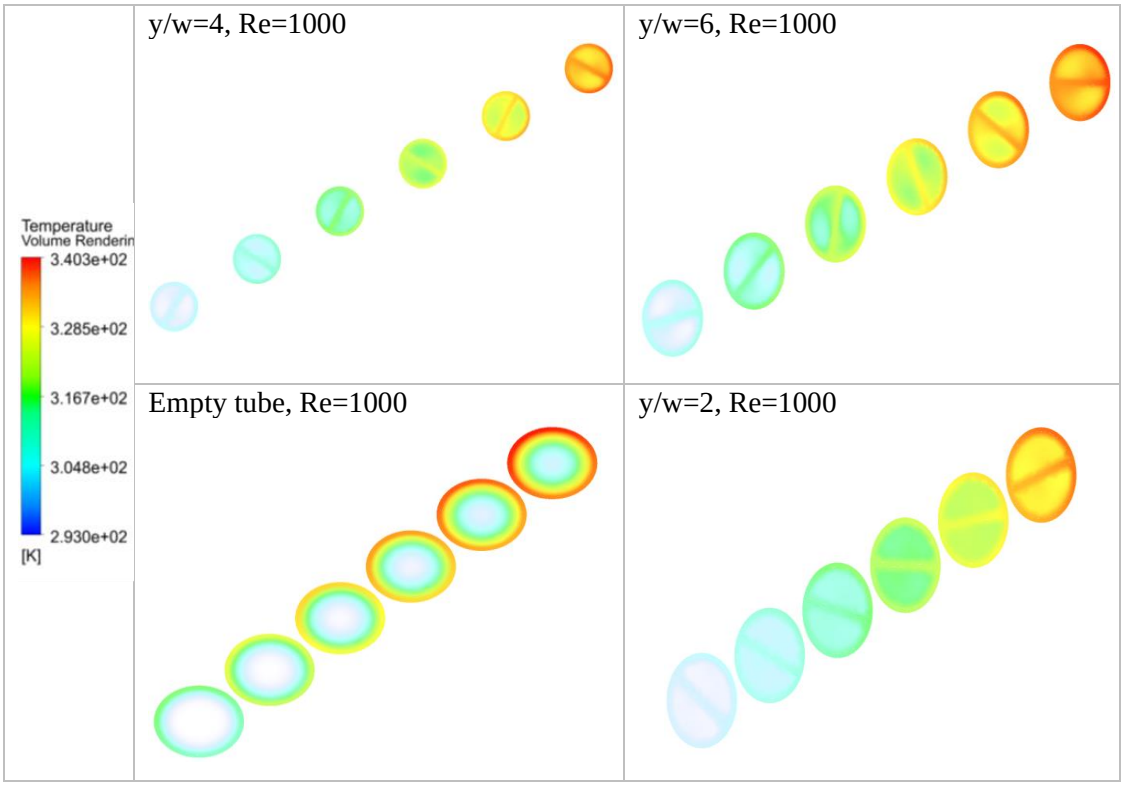
Temperature
Volume Renderin
3.403e+02
3.285e+02
3.167e+02
3.048e+02
2.930e+02
[K]
y/w=4, Re=1000
y/w=6, Re=1000
Empty tube, Re=1000
y/w=2, Re=1000

(b)

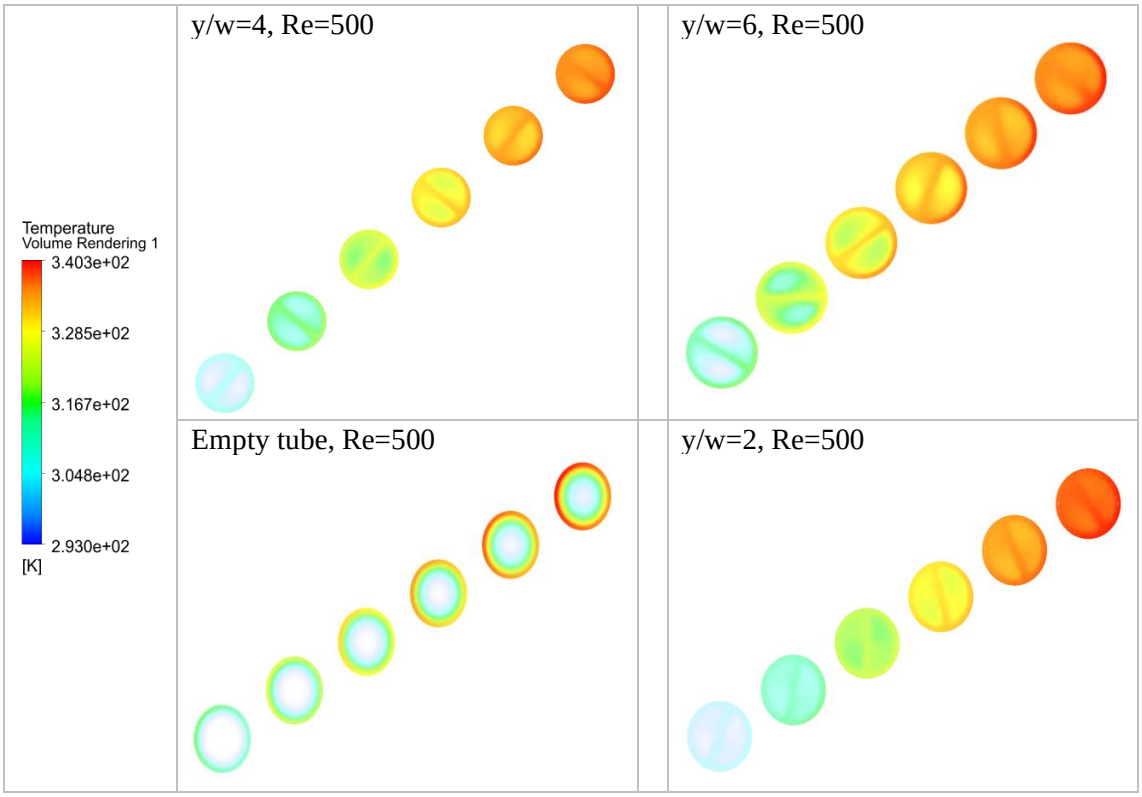

(c)

Figure 5.16. Temperature distribution contours for cases of empty tube and twisted tape inserts y/w (2,4, and 6) at Re 1500 (a),1000 (b), and 500 (c).

Figure 5.15 temperature distribution contours for cases of empty tube and twisted tape inserts y/w (2,4, and 6) at Re 1500 (a) 1000 (b), and 500 (c). Figure 5.15 shows the cross-sectional temperature contours on the outlet temperature for empty tube and twisted tape inserts y/w = 2, 4, 6 for Re=1500, 1000, 500. The temperature contours illustrate the thermal boundary layer's development as it should for the tube's outlet, however as the twisted tape is inserted into the tube and heat transport between the fluid and heated wall, the thermal boundary layer disturbance increases and becomes thinner. The twisted tape improves heat transfer from the wall to the fluid by increasing the efficiency of heat dissipation. Can be seen in this figure is that the presence of twisted tape and lowering its Re value it increases the external fluid outlet temperature to slow down the fluid velocity and thus more heat transfer. As can be seen, twisted tape y/w=2 at a higher temperature distribution for Re (500, 1000, and 1500) with outlet temperature (343K) successively compared to others.

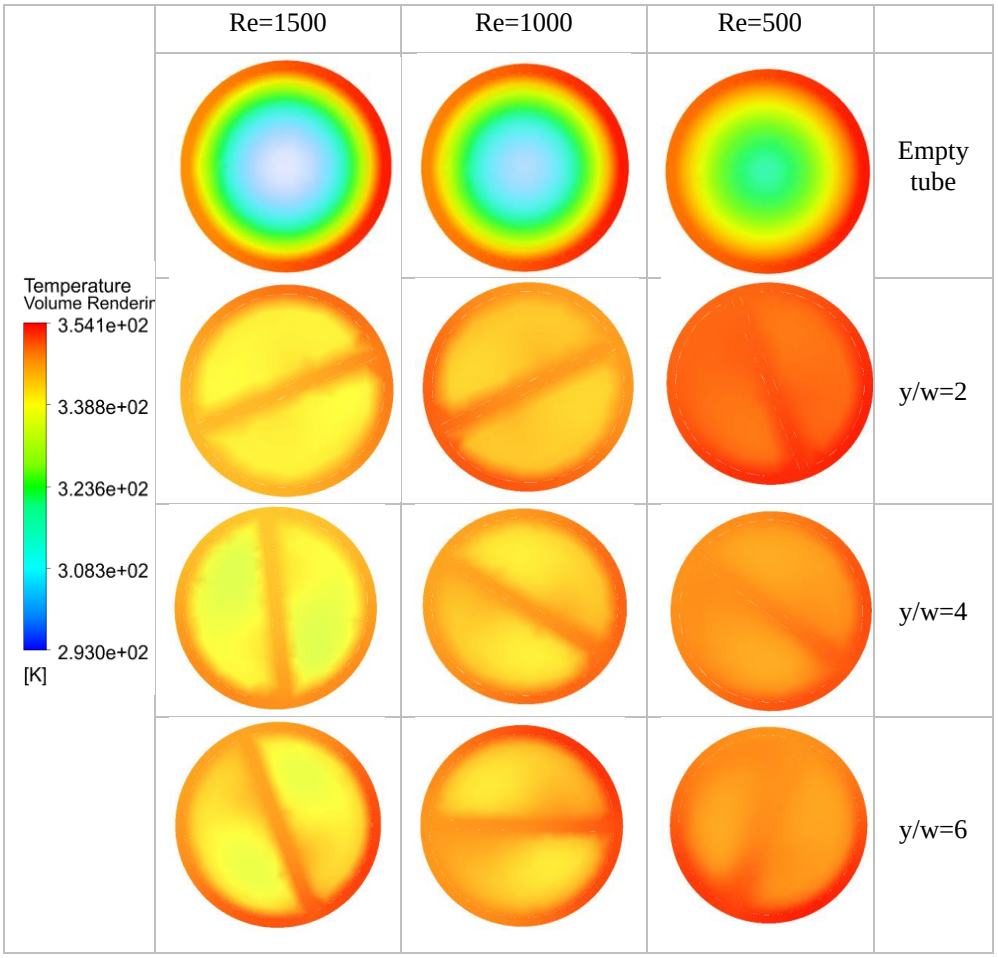

Figure 5.17. Cross-sectional outlet temperature contours for empty tube and twisted ratio y/w =2,4, and 6 for Re=500, 1000, 1500.

Figure 5.16 shows the thermal efficiency of the twisted tape inserts, a variety of performance evaluation criteria have been proposed, to assess whether the performance obtained with the insert is better to that obtained without the insert. The model ANSYS FLUENT data design modeller had been used to sketch the absorber tube with a twisted tape inserted. Heat exchanger systems widely employ the performance evaluation criterion provided by Eq. (4.3). Figure 5.6 depicts the variation of the thermal efficiency for a model with twisted tape insert is Re (500,1000, and 1500). In this study, the thermal efficiency for each twisted tape was illustrating the values of thermal efficiency in terms of cases empty tube and twisted tape inserts y/w (2,4, and 6) is Reynolds number (500,1000, and 1500) values found range between (10% to 21%). The assessment of thermal efficiency, however, offers a useful way to compare enhanced and non-enhanced systems in heat transfer systems. The figure

illustrates that twisted tape inserts y/w (2,4, and 6) achieve higher thermal efficiencies than an empty tube. The heat transfer enhancement plays a significant role in improves the performance. From the results, it shows that the optimum twisted tape y/w=2 at a higher thermal efficiency for the Reynolds number is 1500 is (21%), compared to others.

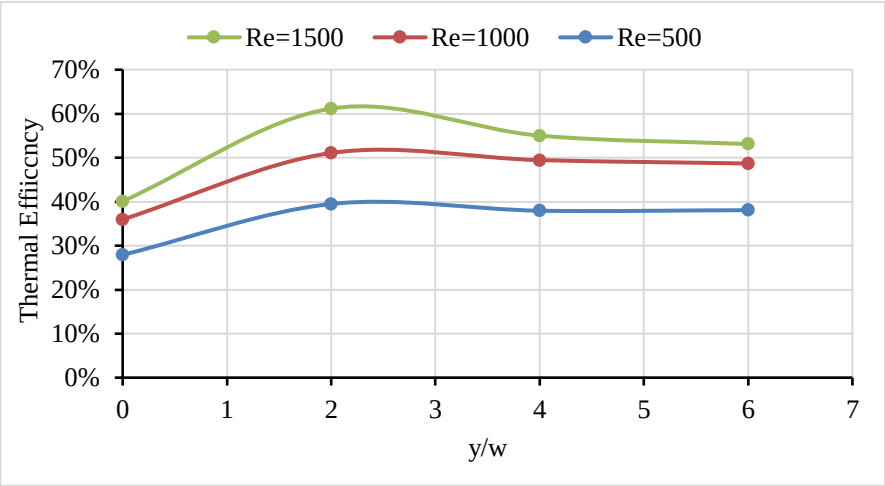

Figure 5.18. Variation ANSYS FLUENT data of the thermal efficiency for different four cases empty tube and twisted tape inserts y/w (2,4, and 6) at Re (500,1000, and 1500).

Figure 5.17. A similar comparison is illustrated the current numerical results for the thermal efficiency through collector at twisted tape inserts had been used to scheme the absorber tube. Figure 5.17 depicts the variation of the thermal efficiency for a model with twisted tape insert is Re (500,1000, and 1500). In this study, the thermal efficiency for each twisted tape was illustrating the values of thermal efficiency in terms of cases empty tube and twisted tape inserts y/w (2,4, and 6) is Reynolds number (500,1000, and 1500). values obtained are in the range of (7% to 21%). Significant gains in thermal efficiency are achieved at twisted tape inserts, as shown by the figure. y/w (2,4, and 6) better than an empty tube. And a key factor in raising performance is the improvement of heat transmission. From the results, it shows that the optimum twisted tape y/w=2 at a higher thermal efficiency for the Reynolds Number is 1500 is (21%), compared to others.

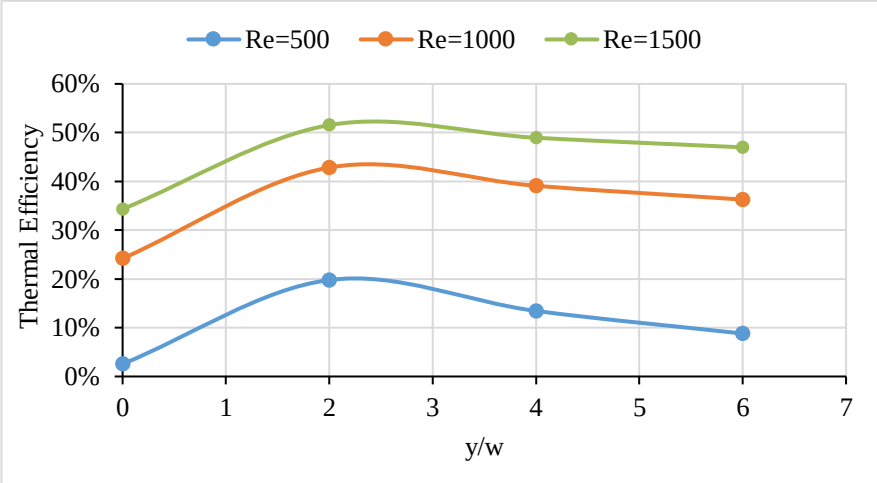

Figure 5.19. Variation the numerical of the thermal efficiency for different four cases empty tube and twisted tape inserts y/w (2,4, and 6) at Re (1500,1000, and 500).

Table 5.1 shows some of previous studies on laminar flow with twisted tapes and their results, the results go parallel with ANSYS FLUENT computational fluid dynamics (CFD) results. where the best result was when twisted tapes ratio is lower for example y/w (2,2.5). Where that the Nu increases with Re increment while friction factor decreases.

Table 5.1. Experimental twisted tape inserted laminar flow studies.

	Y/w	Re	Nu	Friction factor	Mythology
Wongcharee et al. [142]	3	830	13	0.42	Laminar water flow, Copper tube (length 1m, inner diameter 0.019m, outlet diameter 0.022m), aluminium twisted tape(width 18mm, thickness 1mm).
		1000	15	0.39	
		1500	23	0.36	
	4	830	10	0.34	
		1000	13	0.32	
		1500	18	0.3	
	5	830	9	0.3	
		1000	11	0.28	
		1500	16	0.25	
Lim et al. [143]	2.5	500	11.5	0.4	Laminar water flow, Copper tube (length 0.8m, inner diameter 0.0734m, outlet diameter 0.0942m), stainless steel twisted tape(width
		1000	18	0.15	
		1300	19	0.1	
	4	500	12	0.36	
		1000	15.5	0.13	
		1300	17	0.08	

	6	500	12	0.26	5.23mm, thickness 0.84mm, length 800mm).
		1000	14	0.12	
		1300	14.5	0.08	
Syed Jafar et al. [105]	2	946	10	0.0821	Laminar water flow, Copper tube (length 2m, inner diameter 0.012m, outlet diameter 0.0125m), aluminium twisted tape (width 11mm, thickness 1.5mm, length 2000mm).
		1418	12.85	0.0611	
	3	710	8.96	0.0918	
		1654	12.39	0.0619	
	4	946	7.6	0.0791	
		1418	9.57	0.056	
Current study	2	500	9	0.28	
		1000	19.83	0.176	
		1500	31.47	0.134	
	4	500	6.27	0.184	
		1000	13.82	0.11	
		1500	21.93	0.083	
	6	500	5.08	0.17	
		1000	11.18	0.097	
		1500	17.75	0.073	

PART 6

CONCLUSION

In this study, the usable heat gain comes from solar intensity falling on PTC reflected, to the absorber tube, filled with a pure water, and twisted tape inserts tube with $\frac{y}{w} = 2, 4,$ and 6, compared with empty tube in laminar flow, using commercial ANSYS FLUENT (CFD) software tool with actual heat flux profiles coupled. The model allows to predict the thermal efficiency of PTC when a twisted tape inserts is utilized to improve performance. The results showed that, due to the increased surface area and swirling motion caused by the twisted tape insert, the Nu, friction factor, average pressure, and thermal efficiency increase in comparison to those associated with an empty tube. The Nu increased with the increase of Re (500,1000, and 1500) for twisted tape inserts y/w (2,4, and 6) compared to the empty tube where:

- Nusselt number increased (73% at Re=500) (83% at Re=1000) (87% at Re=1500) for use of the twisted tape inserts y/w=2 than empty tube.
- Nusselt number increased (61% at Re=500) (75% at Re=1000) (81% at Re=1500) for use of the twisted tape inserts y/w=4 than empty tube.
- Nusselt number increased (53% at Re=500) (69% at Re=1000) (76% at Re=1500) for use of the twisted tape inserts y/w=6 than empty tube.

The friction factor for the inner surface of the tube increased with the increase of Re (500,1000, and 1500) for twisted tape inserts y/w (2,4, and 6) compared to the empty tube where:

- Friction factor increased (82% at Re=500) (85% at Re=1000) (87% at Re=1500) for use of the twisted tape inserts y/w=2 than empty tube.
- Friction factor increased (72% at Re=500) (76% at Re=1000) (78% at Re=1500) for use of the twisted tape inserts y/w=4 than empty tube.

- Friction factor increased (70% at Re=500) (73% at Re=1000) (75% at Re=1500) for use of the twisted tape inserts y/w=6 than empty tube.

The Thermal efficiency increased with the increase of Re (500,1000, and 1500) for twisted tape inserts y/w (2,4, and 6) compared to the empty tube, and at the lowest flow rates, the increase in the thermal efficiency is remarkable where:

- Thermal efficiency increased (17% at Re=500) (19% at Re=1000) (21% at Re=1500) for use of the twisted tape inserts y/w=2 than empty tube.
- Thermal efficiency increased (11% at Re=500) (14% at Re=1000) (15% at Re=1500) for use of the twisted tape inserts y/w=4 than empty tube.
- Thermal efficiency increased (7% at Re=500) (12% at Re=1000) (13% at Re=1500) for use of the twisted tape inserts y/w=6 than empty tube.

We may conclude from this work that, under certain circumstances, a twisted tape insert is an effective approach to increase the heat transfer between the thermal fluid and the absorber tube surface by creating a swirling flow in a PTC. The research's findings give researchers working in this field a foundation for greater performance based on energy savings in accordance with both heat transfer improvements.

The usage of twisted tape gives good results in heat transfer process, in future works it is good thing to implement different types of tape and study their effect in heat transfer.

PART 7

SUMMARY

In this study, were performed numerical CFD ANSYS FLUENT simulation model by using various cases twisted tape inserted y/w=2,4, and 6 in solar parabolic trough collectors PTC, filled with a pure water, and compared with empty tube. The given results showed that the thermal performance of all cases with various twisted tapes is better than empty tube. And the obtained indicated that in the presence of a twisted tape insert, Nu, average pressure, friction factor, and the thermal efficiency increase with respect to the ones associated to an empty tube, because of increased surface area, and due swirling motion. Nu increased with the increase of Re for twisted tape inserts y/w (2,4, and 6) compared to the empty tube.

REFERENCES

1. Qazi, A., Hussain, F., Rahim, N. A. B. D., Hardaker, G., Alghazzawi, D., Shaban, K., and Haruna, K., "Towards Sustainable Energy: A Systematic Review of Renewable Energy Sources, Technologies, and Public Opinions", ***IEEE Access***, 7: 63837–63851 (2019).

2. Choudhary, K., Jakhar, S., Gakkhar, N., and Sangwan, K. S., "Comparative Life Cycle Assessments of Photovoltaic Thermal Systems with Earth Water Heat Exchanger Cooling", ***Procedia CIRP***, 105: 255–260 (2022).

3. Saleh, A. M., Haris, A., and Ahmad, N., "Towards a UTAUT-Based Model for the Intention to use Solar Water Heaters by Libyan Households", ***International Journal Of Energy Economics And Policy***, 4 (1): 26–31 (2014).

4. Lucas, H., Pinnington, S., and Cabeza, L. F., "Education and training gaps in the renewable energy sector", ***Solar Energy***, 173: 449–455 (2018).

5. Trop, P. and Goricanec, D., "Comparisons between energy carriers' productions for exploiting renewable energy sources", ***Energy***, 108: 155–161 (2015).

6. Mardani, A., Jusoh, A., Zavadskas, E., Cavallaro, F., and Khalifah, Z., "Sustainable and Renewable Energy: An Overview of the Application of Multiple Criteria Decision Making Techniques and Approaches", ***Sustainability***, 7 (10): 13947–13984 (2015).

7. Kousksou, T., Bruel, P., Jamil, A., El Rhafiki, T., and Zeraouli, Y., "Energy storage: Applications and challenges", ***Solar Energy Materials And Solar Cells***, 120: 59–80 (2014).

8. Stigka, E. K., Paravantis, J. A., and Mihalakakou, G. K., "Social acceptance of renewable energy sources: A review of contingent valuation applications", ***Renewable And Sustainable Energy Reviews***, 32: 100–106 (2014).

9. Tsagarakis, K. P., Mavragani, A., Jurelionis, A., Prodan, I., Andrian, T., Bajare, D., Korjakins, A., Magelinskaite-Legkauskiene, S., Razvan, V., and Stasiuliene, L., "Clean vs. Green: Redefining renewable energy. Evidence from Latvia, Lithuania, and Romania", ***Renewable Energy***, 121: 412–419 (2018).

10. Borovik, M. R. and Albers, J. D., "Participation in the Illinois solar renewable energy market", ***The Electricity Journal***, 31 (2): 33–39 (2018).

11. Bayulgen, O. and Benegal, S., "Green Priorities: How economic frames affect perceptions of renewable energy in the United States", ***Energy Research & Social Science***, 47: 28–36 (2019).

12. Keramitsoglou, K. M., Mellon, R. C., Tsagkaraki, M. I., and Tsagarakis, K. P., "Clean, not green: The effective representation of renewable energy", ***Renewable And Sustainable Energy Reviews***, 59: 1332–1337 (2016).

13. Sen, S., Ganguly, S., Das, A., Sen, J., and Dey, S., "Renewable energy scenario in India: Opportunities and challenges", ***Journal Of African Earth Sciences***, 122: 25–31 (2016).

14. Kankam, S. and Boon, E. K., "Energy delivery and utilization for rural development: Lessons from Northern Ghana", ***Energy For Sustainable Development***, 13 (3): 212–218 (2009).

15. Gong, J., Li, C., and Wasielewski, M. R., "Advances in solar energy conversion", ***Chemical Society Reviews***, 48 (7): 1862–1864 (2019).

16. Rabaia, M. K. H., Abdelkareem, M. A., Sayed, E. T., Elsaid, K., Chae, K. J., Wilberforce, T., and Olabi, A. G., "Environmental impacts of solar energy systems: A review", ***Science Of The Total Environment***, 754: (2021).

17. Hayat, M. B., Ali, D., Monyake, K. C., Alagha, L., and Ahmed, N., "Solar energy-A look into power generation, challenges, and a solar-powered future", ***International Journal Of Energy Research***, 43 (3): 1049–1067 (2019).

18. Deceased, J. A. D. and Beckman, W. A., "Solar Engineering of Thermal Processes", 4. Ed., ***Wiley***, New Jersey, 1–20 (2013).

19. Klevinskis, A. and Bučinskas, V., "Analysis of a Flat-Plate Solar Collector", ***Mokslas - Lietuvos Ateitis***, 3: 39–43 (2011).

20. Kalogirou, S. A., "Solar thermal collectors and applications", ***Progress In Energy And Combustion Science***, 30 (3): 231–295 (2004).

21. Prasher, R., "Thermal radiation in dense nano- and microparticulate media", ***Journal Of Applied Physics***, 102 (7): 074316 (2007).

22. Hirsch, L. R., Stafford, R. J., Bankson, J. A., Sershen, S. R., Rivera, B., Price, R. E., Hazle, J. D., Halas, N. J., and West, J. L., "Nanoshell-mediated near-infrared thermal therapy of tumors under magnetic resonance guidance", ***Proceedings Of The National Academy Of Sciences***, 100 (23): 13549–13554 (2003).

23. Liu, G. L., Kim, J., Lu, Y. U., and Lee, L. P., "Optofluidic control using photothermal nanoparticles", ***Nature Materials***, 5 (1): 27–32 (2006).

24. Harris, N., Ford, M. J., and Cortie, M. B., "Optimization of plasmonic heating by gold nanospheres and nanoshells", ***Journal Of Physical Chemistry B***, 110 (22): 10701–10707 (2006).

25. Ghritlahre, H. K. and Prasad, R. K., "Application of ANN technique to predict the performance of solar collector systems - A review", ***Renewable And Sustainable Energy Reviews***, 84: 75–88 (2018).

26. Jaisankar, S., Ananth, J., Thulasi, S., Jayasuthakar, S. T., and Sheeba, K. N., "A comprehensive review on solar water heaters", ***Renewable And Sustainable Energy Reviews***, 15 (6): 3045–3050 (2011).

27. Nagarajan, P. K., Subramani, J., Suyambazhahan, S., and Sathyamurthy, R., "Nanofluids for solar collector applications: A review", ***Energy Procedia***, 61: 2416–2434 (2014).

28. Islam, M. T., Huda, N., Abdullah, A. B., and Saidur, R., "A comprehensive review of state-of-the-art concentrating solar power (CSP) technologies: Current status and research trends", ***Renewable And Sustainable Energy Reviews***, 91: 987–1018 (2018).

29. Sheikholeslami, M., Gorji-bandpy, M., and Domiri, D., "Review of heat transfer enhancement methods : Focus on passive methods using swirl fl ow devices", ***Renewable And Sustainable Energy Reviews***, 49: 444–469 (2015).

30. Manikandan, G. K., Iniyan, S., and Goic, R., "Enhancing the optical and thermal efficiency of a parabolic trough collector – A review", ***Applied Energy***, 235: 1524–1540 (2019).

31. Eiamsa-ard, S., Thianpong, C., and Eiamsa-ard, P., "Turbulent heat transfer enhancement by counter/co-swirling flow in a tube fitted with twin twisted tapes", ***Experimental Thermal And Fluid Science***, 34 (1): 53–62 (2010).

32. Ravi Kumar, K. and Reddy, K. S., "Effect of porous disc receiver configurations on performance of solar parabolic trough concentrator", ***Heat And Mass Transfer/Waerme- Und Stoffuebertragung***, 48 (3): 555–571 (2012).

33. Muñoz, J. and Abánades, A., "Analysis of internal helically finned tubes for parabolic trough design by CFD tools", ***Applied Energy***, 88 (11): 4139–4149 (2011).

34. Cheng, Z. D., He, Y. L., and Cui, F. Q., "Numerical study of heat transfer enhancement by unilateral longitudinal vortex generators inside parabolic trough solar receivers", ***International Journal Of Heat And Mass Transfer***, 55 (21–22): 5631–5641 (2012).

35. Kasperski, J. and Nem, M., "Investigation of thermo-hydraulic performance of concentrated solar air-heater with internal multiple- fi n array", ***Applied Thermal Engineering***, 58 (1): 411–419 (2013).

36. Ghadirijafarbeigloo, S., Zamzamian, A. H., and Yaghoubi, M., "3-D numerical simulation of heat transfer and turbulent flow in a receiver tube of solar parabolic trough concentrator with louvered twisted-tape inserts", ***Energy Procedia***, 49:

373–380 (2014).

37. Song, X., Dong, G., Gao, F., Diao, X., Zheng, L., and Zhou, F., "A numerical study of parabolic trough receiver with nonuniform heat flux and helical screw-tape inserts", ***Energy***, 77: 771–782 (2014).

38. Mwesigye, A., Bello-Ochende, T., and Meyer, J. P., "Heat transfer and thermodynamic performance of a parabolic trough receiver with centrally placed perforated plate inserts", ***Applied Energy***, 136: 989–1003 (2014).

39. Huang, Z., Yu, G. L., Li, Z. Y., and Tao, W. Q., "Numerical Study on Heat Transfer Enhancement in a Receiver Tube of Parabolic Trough Solar Collector with Dimples, Protrusions and Helical Fins", ***Energy Procedia***, 69: 1306–1316 (2015).

40. Bellos, E., Tzivanidis, C., Antonopoulos, K. A., and Gkinis, G., "Thermal enhancement of solar parabolic trough collectors by using nanofluids and converging-diverging absorber tube", ***Renewable Energy***, 94: 213–222 (2016).

41. Zhu, X., Zhu, L., and Zhao, J., "Wavy-tape insert designed for managing highly concentrated solar energy on absorber tube of parabolic trough receiver", ***Energy***, 141: 1146–1155 (2017).

42. Zheng, N., Liu, W., Liu, Z., Liu, P., and Shan, F., "A numerical study on heat transfer enhancement and the flow structure in a heat exchanger tube with discrete double inclined ribs", ***Applied Thermal Engineering***, 90: 232–241 (2015).

43. Raj, A., Suri, S., Kumar, A., and Maithani, R., "Experimental determination of enhancement of heat transfer in a multiple square perforated twisted tape inserts heat exchanger tube", ***Experimental Heat Transfer***, 00 (00): 1–21 (2017).

44. Shabanian, S. R., Rahimi, M., Shahhosseini, M., and Alsairafi, A. A., "CFD and experimental studies on heat transfer enhancement in an air cooler equipped with different tube inserts", ***International Communications In Heat And Mass Transfer***, 38 (3): 383–390 (2011).

45. Muñoz-Esparza, D. and Sanmiguel-Rojas, E., "Numerical simulations of the laminar flow in pipes with wire coil inserts", ***Computers And Fluids***, 44 (1): 169–177 (2011).

46. Kurtbaş, I., Gülçimen, F., Akbulut, A., and Buran, D., "Heat transfer augmentation by swirl generators inserted into a tube with constant heat flux", ***International Communications In Heat And Mass Transfer***, 36 (8): 865–871 (2009).

47. Pawar, V. R. and Sobhansarbandi, S., "CFD modeling of a thermal energy storage based heat pipe evacuated tube solar collector", ***Journal Of Energy Storage***, 30: (2020).

48. Aggarwal, S., Kumar, R., Kumar, S., Bhatnagar, M., and Kumar, P., "Computational fluid dynamics based analysis for optimization of various thermal enhancement techniques used in evacuated tubes solar collectors: A review", ***Materials Today: Proceedings***, 46: 8700–8707 (2021).

49. Emam, M. A. El, Zhou, L., Shi, W., Han, C., Bai, L., and Agarwal, R., "Theories and Applications of CFD – DEM Coupling Approach for Granular Flow : A Review", Archives of Computational Methods in Engineering, ***Springer Netherlands***, (2021).

50. Yang, Y., Wang, S., and Wen, C., "Gas-liquid two-phase flows in double inlet cyclones for natural gas separation", ***Cogent Engineering***, 4 (1): 1–10 (2017).

51. Romaní Fernández, X. and Nirschl, H., "Simulation of particles and sediment behaviour in centrifugal field by coupling CFD and DEM", ***Chemical Engineering Science***, 94: 7–19 (2013).

52. Wang, Y., Williams, K., Jones, M., and Chen, B., "CFD Simulation Methodology for Gas-solid Flow in Bypass", ***Applied Thermal Engineering***, (2017).

53. Ullah, A., Hong, K., Gao, Y., Gungor, A., and Zaman, M., "An overview of Eulerian CFD modeling and simulation of non-spherical biomass particles", ***Renewable Energy***, 141: 1054–1066 (2019).

54. Heris, S. Z., Esfahany, M. N., and Etemad, G., "Numerical investigation of nanofluid laminar convective heat transfer through a circular tube", ***Numerical Heat Transfer; Part A: Applications***, 52 (11): 1043–1058 (2007).

55. He, Y., Men, Y., Zhao, Y., Lu, H., and Ding, Y., "Numerical investigation into the convective heat transfer of TiO2 nanofluids flowing through a straight tube under the laminar flow conditions", ***Applied Thermal Engineering***, 29 (10): 1965–1972 (2009).

56. Bianco, V., Chiacchio, F., Manca, O., and Nardini, S., "Numerical investigation of nanofluids forced convection in circular tubes", ***Applied Thermal Engineering***, 29 (17–18): 3632–3642 (2009).

57. Muhammad, T., Alamri, S. Z., Waqas, H., and Habib, D., "Bioconvection flow of magnetized Carreau nanofluid under the influence of slip over a wedge with motile microorganisms", ***Journal Of Thermal Analysis And Calorimetry***, (0123456789): (2020).

58. Nabavi, M., Elveny, M., Danshina, S. D., Behroyan, I., and Babanezhad, M., "Velocity prediction of Cu/water nanofluid convective flow in a circular tube: Learning CFD data by differential evolution algorithm based fuzzy inference system (DEFIS)", ***International Communications In Heat And Mass Transfer***, 126: (2021).

59. Jaramillo, O. A., Borunda, M., Velazquez-Lucho, K. M., and Robles, M., "Parabolic trough solar collector for low enthalpy processes: An analysis of the efficiency enhancement by using twisted tape inserts", ***Renewable Energy***, 93: 125–141 (2016).

60. Eiamsa-ard, S. and Wongcharee, K., "Convective heat transfer enhancement using Ag-water nanofluid in a micro-fin tube combined with non-uniform twisted tape", ***International Journal Of Mechanical Sciences***, 146–147: 337–354 (2018).

61. Ayinde, T. F., "A generalized relationship for swirl decay in laminar pipe flow", ***Sadhana - Academy Proceedings In Engineering Sciences***, 35 (2): 129–137 (2010).

62. Eiamsa-ard, S., Seemawute, P., and Wongcharee, K., "Influences of peripherally-cut twisted tape insert on heat transfer and thermal performance characteristics in laminar and turbulent tube flows", ***Experimental Thermal And Fluid Science***, 34 (6): 711–719 (2010).

63. Sadhishkumar, S. and Balusamy, T., "Performance improvement in solar water heating systems - A review", ***Renewable And Sustainable Energy Reviews***, 37: 191–198 (2014).

64. Mwesigye, A., Bello-Ochende, T., and Meyer, J. P., "Heat transfer and entropy generation in a parabolic trough receiver with wall-detached twisted tape inserts", ***International Journal Of Thermal Sciences***, 99: 238–257 (2016).

65. Nakhchi, M. E. and Esfahani, J. A., "Numerical investigation of rectangular-cut twisted tape insert on performance improvement of heat exchangers", ***International Journal Of Thermal Sciences***, 138: 75–83 (2019).

66. Rahimi, M., Shabanian, S. R., and Alsairafi, A. A., "Experimental and CFD studies on heat transfer and friction factor characteristics of a tube equipped with modified twisted tape inserts", ***Chemical Engineering And Processing: Process Intensification***, 48 (3): 762–770 (2009).

67. Namar, M. M. and Jahanian, O., "Energy and exergy analysis of a hydrogen-fueled HCCI engine", ***Journal Of Thermal Analysis And Calorimetry***, 137 (1): 205–215 (2019).

68. Saysroy, A., Changcharoen, W., and Eiamsa-ard, S., "Performance assessment of turbular heat exchanger tubes containing rectangular-cut twisted tapes with alternate axes", ***Journal Of Mechanical Science And Technology***, 32 (1): 433–445 (2018).

69. Li, W., Khan, T. A., Tang, W., and Minkowycz, W. J., "Numerical study and optimization of corrugation height and angle of attack of vortex generator in the wavy fin-and-tube heat exchanger", ***Journal Of Heat Transfer***, 140 (11): (2018).

70. Sandhu, G., Siddiqui, K., and Garcia, A., "Experimental study on the combined effects of inclination angle and insert devices on the performance of a flat-plate solar collector", ***International Journal Of Heat And Mass Transfer***, 71: 251–263 (2014).

71. Saha, S. K., Dutta, A., and Dhal, S. K., "Friction and heat transfer characteristics of laminar swirl ¯ ow through a circular tube ® tted with regularly spaced twisted-tape elements", ***International Journal Of Heat And Mass Transfer***, 44 (22): 4211–4223 (2001).

72. Jaisankar, S., Radhakrishnan, T. K., and Sheeba, K. N., "Experimental studies on heat transfer and friction factor characteristics of forced circulation solar water heater system fitted with helical twisted tapes", ***Solar Energy***, 83 (11): 1943–1952 (2009).

73. Habeeb, L. J., Saleh, F. A., and Maajel, B. M., "Heat Transfer Enhancement in a Circular Tube Fitted with Passive Technique as Twisted Tape Insert in Turbulent Flow Regime : A Review of the Recent Literature", ***Journal Of Nanoscience***, 1 (4): 43–49 (2015).

74. Hemmat Esfe, M., Mazaheri, H., Mirzaei, S. S., Kashi, E., Kazemi, M., and Afrand, M., "Effects of twisted tapes on thermal performance of tri-lobed tube: An applicable numerical study", ***Applied Thermal Engineering***, 144: 512–521 (2018).

75. Ghalambaz, M., Arasteh, H., Mashayekhi, R., Keshmiri, A., Talebizadehsardari, P., and Yaïci, W., "Investigation of overlapped twisted tapes inserted in a double-pipe heat exchanger using two-phase nanofluid", ***Nanomaterials***, 10 (9): 1–17 (2020).

76. Hamzah, D. A. and Al-Farhany, K., "Effect of twisted tape ratio on the solar generator half-length pipe", ***International Journal Of Heat And Technology***, 37 (2): 407–412 (2019).

77. Nakhchi, M. E. and Esfahani, J. A., "Sensitivity analysis of a heat exchanger tube fitted with cross-cut twisted tape with alternate axis", ***Journal Of Heat Transfer***, 141 (4): (2019).

78. Venkatesan, S. P., Annamalai, S., Arun, S., Purusothaman, M., Hemanandh, J., and Ganesan, S., "Thermal performance of single glazing V-through solar collector using horizontal and vertical nail cut twisted tape insert", ***AIP Conference Proceedings***, 2311: (2020).

79. Arjmandi, H., Amiri, P., and Saffari Pour, M., "Geometric optimization of a double pipe heat exchanger with combined vortex generator and twisted tape: A CFD and response surface methodology (RSM) study", ***Thermal Science And Engineering Progress***, 18: (2020).

80. Amani, K., Ebrahimpour, M., Akbarzadeh, S., and Valipour, M. S., "The utilization of conical strip inserts in a parabolic trough collector", ***Journal Of Thermal Analysis And Calorimetry***, 140 (3): 1625–1631 (2020).

81. Afsharpanah, F., Sheshpoli, A. Z., Pakzad, K., Soheil, S., and Ajarostaghi, M., "Numerical Investigation Of Non-Uniform Heat Transfer Enhancement In Parabolic Trough Solar Collectors Using Dual Modified Twisted-Tape Inserts", ***Journal Of Thermal Engineering***, 7 (1): 133–147 (2021).

82. Al-Obaidi, A. R. and Alhamid, J., "Investigation of thermo-hydraulics flow and augmentation of heat transfer in the circular pipe by combined using corrugated tube with dimples and fitted with varying tape insert configurations", ***International Journal Of Heat And Technology***, 39 (2): 365–374 (2021).

83. Arasteh, H., Rahbari, A., Mashayekhi, R., Keshmiri, A., Mahani, R. B., and Talebizadehsardari, P., "Effect of pitch distance of rotational twisted tape on the heat transfer and fluid flow characteristics", ***International Journal Of Thermal Sciences***, 170: (2021).

84. Azizi, Z., Rostampour, V., Jafarmadar, S., Khorasani, S., and Abdzadeh, B., "Performance evaluation of horizontal straight tube equipped with twisted tape turbulator, with air–water two-phase flow as working fluid", ***Journal Of Thermal Analysis And Calorimetry***, 147 (6): 4339–4353 (2022).

85. Dandoutiya, B. K. and Kumar, A., "CFD analysis for the performance improvement of a double pipe heat exchanger with twisted tape having triangular cut", ***Energy Sources, Part A: Recovery, Utilization And Environmental Effects***, (2021).

86. Kumar, R., Nandan, G., Dwivedi, G., Kumar Shukla, A., and Shrivastava, R., "Modeling of triangular perforated twisted tape with V-Cuts in double pipe heat exchanger", ***Materials Today: Proceedings***, 46: 5389–5395 (2020).

87. Rawani, A., Sharma, S. P., and Singh, K. D. P., "Enhancement in performance of parabolic trough collector with serrated twisted-tape inserts", ***International Journal Of Thermodynamics***, 20 (2): 111–119 (2017).

88. Bellos, E. and Tzivanidis, C., "Enhancing the performance of evacuated and non-evacuated parabolic trough collectors using twisted tape inserts, perforated plate inserts and internally finned absorber", ***Energies***, 11 (5): (2018).

89. Hayat, M. Z., Nandan, G., Tiwari, A. K., Sharma, S. K., Shrivastava, R., and Singh, A. K., "Numerical study on heat transfer enhancement using twisted tape with trapezoidal ribs in an internal flow", ***Materials Today: Proceedings***, 46: 5412–5419 (2020).

90. Ju, Y., Zhu, T., Mashayekhi, R., Mohammed, H. I., Khan, A., Talebizadehsardari, P., and Yaïci, W., "Evaluation of Multiple Semi-Twisted Tape Inserts in a Heat Exchanger Pipe Using Al2O3 Nanofluid", ***Nanomaterials***, 11 (6): 1570 (2021).

91. Raheem, A., Siddique, W., Farooqui, Z. H., Salameh, T., Haq, I., Waheed, K., and Qureshi, K., "Performance evaluation of adding Helical-screw Tape Inserts in Parabolic Solar Trough Collectors as a Source of Cleaner Energy Production", ***Journal Of Cleaner Production***, 297: 126628 (2021).

92. Saedodin, S., Zaboli, M., and Mousavi Ajarostaghi, S. S., "Hydrothermal analysis of heat transfer and thermal performance characteristics in a parabolic trough solar collector with Turbulence-Inducing elements", ***Sustainable Energy Technologies And Assessments***, 46: 101266 (2021).

93. Thakur, A., Kumar, S., Kumar, P., Kumar, S., and Bhardwaj, A. K., "A review on the simulation/CFD based studies on the thermal augmentation of flat plate solar collectors", ***Materials Today: Proceedings***, 46: 8578–8585 (2021).

94. Kundan, L. and Darshan, M. B., "Performance investigation of a concentric double tube heat exchanger using twisted tape inserts and nanofluid", ***Particulate Science And Technology***, 40 (3): 307–324 (2022).

95. Mashayekhi, R., Arasteh, H., Talebizadehsardari, P., Kumar, A., Hangi, M., and Rahbari, A., "Heat Transfer Enhancement of Nanofluid Flow in a Tube Equipped with Rotating Twisted Tape Inserts: A Two-Phase Approach", ***Heat Transfer Engineering***, 43 (7): 608–622 (2022).

96. Sarviya, R. M. and Fuskele, V., "Heat Transfer and Pressure Drop in a Circular Tube Fitted with Twisted Tape Insert Having Continuous Cut Edges", ***Journal Of Energy Storage***, 19: 10–14 (2018).

97. Rezaei, O., Akbari, O. A., Marzban, A., Toghraie, D., Pourfattah, F., and Mashayekhi, R., "The numerical investigation of heat transfer and pressure drop of turbulent flow in a triangular microchannel", ***Physica E: Low-Dimensional Systems And Nanostructures***, 93: 179–189 (2017).

98. Yang, D., Khan, T. S., Al-Hajri, E., Ayub, Z. H., and Ayub, A. H., "Geometric optimization of shell and tube heat exchanger with interstitial twisted tapes outside the tubes applying CFD techniques", ***Applied Thermal Engineering***, 152: 559–572 (2019).

99. Kumar, A. and Prasad, B. N., "Investigation of twisted tape inserted solar water heaters - Heat transfer, friction factor and thermal performance results", ***Renewable Energy***, 19 (3): 379–398 (2000).

100. Hobbi, A. and Siddiqui, K., "Experimental study on the effect of heat transfer enhancement devices in flat-plate solar collectors", ***International Journal Of Heat And Mass Transfer***, 52 (19–20): 4650–4658 (2009).

101. Jaisankar, S., Radhakrishnan, T. K., and Sheeba, K. N., "Studies on heat transfer and friction factor characteristics of thermosyphon solar water heating system with helical twisted tapes", ***Energy***, 34 (9): 1054–1064 (2009).

102. Sekhar, Y. R., Sharma, K. V., Karupparaj, R. T., and Chiranjeevi, C., "Heat transfer enhancement with Al2O3 nanofluids and twisted tapes in a pipe for solar thermal applications", ***Procedia Engineering***, 64: 1474–1484 (2013).

103. Chang, C., Xu, C., Wu, Z. Y., Li, X., Zhang, Q. Q., and Wang, Z. F., "Heat Transfer Enhancement and Performance of Solar Thermal Absorber Tubes with Circumferentially Non-uniform Heat Flux", ***Energy Procedia***, 69: 320–327 (2015).

104. Syed, K., Jafar, J., and Sivaraman, B., "Thermal Performance of Solar Parabolic Trough Collector Using Nanofluids and the Absorber with Nail Twisted Tapes Inserts", ***Nternational Energy Journal***, 14 (4): 189–198 (2014).

105. Syed Jafar K and B, S., "OPTIMIZATION OF PERFORMANCE CHARACTERISTICS IN THE ABSORBER WITH TWISTED TAPES INSERTS OF PARABOLIC TROUGH COLLECTOR USING RESPONSE SURFACE METHODOLOGY", ***ARPN Journal Of Engineering And Applied Sciences***, 10 (8): 3457–3464 (2015).

106. Eiamsa-ard, S. and Promvonge, P., "Enhancement of heat transfer in a tube with regularly-spaced helical tape swirl generators", ***Solar Energy***, 78 (4): 483–494 (2005).

107. Chin, S.-B., Foo, J.-J., Lai, Y.-L., and Yong, T. K.-K., "Forced convective heat transfer enhancement with perforated pin fins", ***Heat And Mass Transfer***, 49 (10): 1447–1458 (2013).

108. Durga Prasad, P. V. and Gupta, A. V. S. S. K. S., "Experimental investigation on enhancement of heat transfer using Al2O3/water nanofluid in a u-tube with twisted tape inserts", ***International Communications In Heat And Mass Transfer***, 75: 154–161 (2016).

109. Guo, J., Fan, A., Zhang, X., and Liu, W., "A numerical study on heat transfer and friction factor characteristics of laminar flow in a circular tube fitted with center-cleared twisted tape", ***International Journal Of Thermal Sciences***, 50 (7): 1263–1270 (2011).

110. Salman, S. D., Kadhum, A. A. H., Takriff, M. S., and Mohamad, A. B., "Heat Transfer Enhancement of Laminar Nanofluids Flow in a Circular Tube Fitted with Parabolic-Cut Twisted Tape Inserts", ***The Scientific World Journal***, 2014: 1–7 (2014).

111. Yadav, R. J. and Padalkar, A. S., "CFD Analysis for Heat Transfer Enhancement inside a Circular Tube with Half-Length Upstream and Half-Length Downstream Twisted Tape", ***Journal Of Thermodynamics***, 2012 (1): 1–12 (2012).

112. El-Said, E. M. S., Abdulaziz, M., and Awad, M. M., "A numerical investigation on heat transfer enhancement and the flow characteristics in a new type plate

heat exchanger using helical flow duct", ***Cogent Engineering***, 4 (1): 1396638 (2017).

113. Bhuyan, M. M., Deb, U. K., Shahriar, M., and Acherjee, S., "Simulation of Heat Transfer in a Tubular Pipe Using Different Twisted Tape Inserts", ***Open Journal Of Fluid Dynamics***, 07 (03): 397–409 (2017).

114. Piriyarungroj, N., Eiamsa-ard, S., Promvonge, P., Eiamsa-Ard, P., and Thianpong, C., "Simulation of Turbulent Heat Transfer in a Tube Fitted with Twisted Tape Placed Separately from the Tube Walls", ***Applied Mechanics And Materials***, 751: 245–250 (2015).

115. Sharifi, K., Sabeti, M., Rafiei, M., Mohammadi, A. H., and Shirazi, L., "Computational fluid dynamics (CFD) technique to study the effects of helical wire inserts on heat transfer and pressure drop in a double pipe heat exchanger", ***Applied Thermal Engineering***, 128: 898–910 (2018).

116. Al-Obaidi, A. R. and Alhamid, J., "The Effect of Different Twisted Tape Inserts Configurations on Fluid Flow Characteristics, Pressure Drop, Thermo-hydraulic Performance and Heat Transfer Enhancement in the 3D Circular Tube", ***International Journal Of Ambient Energy***, 1–24 (2022).

117. Chu, W.-X., Tsai, C.-A., Lee, B.-H., Cheng, K.-Y., and Wang, C.-C., "Computational Fluid Dynamics Study on Heat Transfer Augmentation in Tube With Various V-Cut Twisted Tape", ***Journal Of Heat Transfer***, 144 (6): 062001 (2022).

118. Akram, N., Sadri, R., Kazi, S. N., Ahmed, S. M., Zubir, M. N. M., Ridha, M., Soudagar, M., Ahmed, W., Arzpeyma, M., and Tong, G. B., "An experimental investigation on the performance of a flat-plate solar collector using eco-friendly treated graphene nanoplatelets–water nanofluids", ***Journal Of Thermal Analysis And Calorimetry***, 138 (1): 609–621 (2019).

119. Damarlal Chaudhary, H. and A Namjoshi, D. S., "Experimental Investigation of Inserted Twisted Tape Pitch Effect in Evacuated Solar Water Heater", ***International Journal Of Innovative Research In Engineering & Multidisciplinary Physical Sciences***, 9 (5): 1–1 (2021).

120. Tusar, M., Noman, A., Islam, M., Yarlagadda, P., and Salam, B., "CFD study of heat transfer enhancement and fluid flow characteristics of turbulent flow through tube with twisted tape inserts", ***Energy Procedia***, 160: 715–722 (2019).

121. Alzahrani, S. M., "Computational fluid dynamics modeling and comparison of advanced techniques for heat transfer augmentation for nuclear applications", ***Missouri University Of Science And Technology***, PhD, 98-109 (2019).

122. Karanth, K. V., N, M., Kumar, S., and M.S, M., "Numerical And Experimental Study Of A Solar Water Heater For Enhancement In Thermal Performance", ***International Journal Of Research In Engineering And Technology***, 04 (03): 548–553 (2015).

123. Yao, K., Li, T., Tao, H., Wei, J., and Feng, K., "Performance Evaluation of All-glass Evacuated Tube Solar Water Heater with Twist Tape Inserts Using CFD", ***Energy Procedia***, 70: 332–339 (2015).

124. Jasim, A. K., Freegah, B., and Alhamdo, M. H., "Numerical and experimental analysis of effect of working fluid amount on the thermal performance of thermo-syphon system", ***Materials Science And Engineering***, 928 (2): 022022 (2020).

125. Keen, V. I. and Prajapati, S., "Experimental Analysis of Evacuated Tube Solar Water Heater Using Twisted Tape", ***International Journal Of Emerging Technologies And Innovative Research***, 5 (12): 181–187 (2018).

126. Reddy, G. J. C., "Cfd Analysis and Experimental Investigation Of Heat Transfer And Fluid Flow In A Parabolic Trough Solar Collectorusing Twisted Tape Inserts And Hybrid Nanofluids", ***International Journal Of Emerging Technologies And Innovative Research***, 8 (8): 405–431 (2021).

127. Sunil Yadav and Pooja Tiwari, "Numerical Investigation of Flow and the Heat Transfer Performance of a Circular Collector Tube Ensuring Minimization of Frictional Loss", ***International Journal Of Engineering Research And***, V7 (03): 14–17 (2018).

128. Xue, Y., Ge, Z., Du, X., and Yang, L., "On the Heat Transfer Enhancement of Plate Fin Heat Exchanger", ***Energies***, 11 (6): 1398 (2018).

129. Dehankar, P. B., Joshi, K., Bhosale, V. A., and Mulik, R. N., "Assessment of twist tape thermal performance in heat transfer passive augmentation technique", ***Beni-Suef University Journal Of Basic And Applied Sciences***, 11 (1): 29 (2022).

130. Ghalambaz, M., Mashayekhi, R., Arasteh, H., Ali, H. M., Talebizadehsardari, P., and Yaïci, W., "Thermo-Hydraulic Performance Analysis on the Effects of Truncated Twisted Tape Inserts in a Tube Heat Exchanger", ***Symmetry***, 12 (10): 1–22 (2020).

131. Yılmaz, İ. H., Mwesigye, A., and Göksu, T. T., "Enhancing the overall thermal performance of a large aperture parabolic trough solar collector using wire coil inserts", ***Sustainable Energy Technologies And Assessments***, 39: 100696 (2020).

132. Soteris A. Kalogirou, "Solar Energy Engineering: Processes and Systems", 2. Ed., ***Elsevier Inc.***, 1–819 (2014).

133. Meseguer, J., Pérez-Grande, I., and Sanz-Andrés, A., "Thermal radiation heat transfer", Spacecraft Thermal Control, 1. Ed., ***Woodhead Publishing Limited***, USA, 73-86 (2012).

134. Madadi, V., Tavakoli, T., and Rahimi, A., "First and second thermodynamic law analyses applied to a solar dish collector", ***Journal Of Non-Equilibrium Thermodynamics***, 39 (4): 183–197 (2014).

135. Frank P. Incropera, D. P. D., "Fundamentals of Heat and Mass Transfer", 6. Ed., ***Wiley***, New York, 912 (1998).

136. Fox, R. O., "Computational Models for Turbulent Reacting Flows", ***Cambridge University Press***, 419 (2003).

137. Samutpraphut, B., Eiamsa-ard, S., Chuwattanakul, V., Thianpong, C., Maruyama, N., and Hirota, M., "Influence of sawtooth twisted tape on thermal enhancement of heat exchanger tube", ***Energy Reports***, 9 (1): 696–703 (2023).

138. Geßner, T., "Dynamic Mesh Adaption Detailed Reaction Mechanisms", ***International Series Of Numerical Mathematics***, 140: 415–424 (2001).

139. Iddir, H. and Arastoopour, H., "Modeling of multitype particle flow using the kinetic theory approach", ***AIChE Journal***, 51 (6): 1620–1632 (2005).

140. Olia, H., Torabi, M., Bahiraei, M., Ahmadi, M. H., Goodarzi, M., and Safaei, M. R., "Application of Nanofluids in Thermal Performance Enhancement of Parabolic Trough Solar Collector: State-of-the-Art", ***Applied Sciences***, 9 (3): 463 (2019).

141. Muzychka, Y. and Yovanovich, M., "Modeling Nusselt numbers for thermally developing laminar flow in non-circular ducts", ***7th AIAA/ASME Joint Thermophysics And Heat Transfer Conference***, Reston, Virigina (1998).

142. Wongcharee, K. and Eiamsa-ard, S., "Friction and heat transfer characteristics of laminar swirl flow through the round tubes inserted with alternate clockwise and counter-clockwise twisted-tapes", ***International Communications In Heat And Mass Transfer***, 38 (3): 348–352 (2011).

143. Lim, K. Y., Hung, Y. M., and Tan, B. T., "Performance evaluation of twisted-tape insert induced swirl flow in a laminar thermally developing heat exchanger", ***Applied Thermal Engineering***, 121: 652–661 (2017).

RESUME

Nasseer Sabbeeh Jaralleh is a Mechanical Engineer. Graduated from the Faculty of Engineering, Technology University/ Iraq. He obtained a Bachelor's degree in 2000. I work as a government employee for the Iraqi Media Network since 2002. Currently studying for a master's degree at Karabuk University in the field of Mechanical Systems Engineering.